Supporting Information

Engineering a Highly Selective Probe for Ratiometric Imaging H_2S_n and Revealing its Signaling Pathway in Fatty Liver Disease

Wei Li,[‡a] Lu Wang,[‡b] Shulu Yin,[a] Huanhua Lai,[a] Lin Yuan,*[, a] Xiaobing Zhang[a]

[a] State Key Laboratory of Chemo/Biosensing and Chemometrics, College of Chemistry and Chemical Engineering, Hunan University, Changsha 410082, P. R. China

[b] Department of Chemical Biology, Max Planck Institute for Medical Research, Jahnstrasse 29, Heidelberg 69120, Germany

[‡] These authors contributed equally

* E-mail: lyuan@hnu.edu.cn

Table of Contents:

1. Supplemental Experimental Procedures

Materials and instruments. All chemical reagents for synthesis were obtained from commercial suppliers and were used in whole experiment without further purification, and solvents used were purified by standard methods before using. Na_2S_2 and Na_2S_4 were gifts from professor Ming Xian, Washington State University, United States. The water used in the whole experiment was twice-distilled water. ^1H NMR and ^{13}C NMR spectra were recorded on a Bruker-400 spectrometer with an internal standard (TMS). Mass spectra were performed using an LCQ Advantage ion trap mass spectrometer from Thermo Finnigan. High-resolution electron spray mass spectra (HRMS) were obtained from ESI/Q-TOF Micro TM HRMS (Zhengzhou University Analysis and Testing Center). Absorption and fluorescence spectroscopic studies were performed in a UV-1800 ultraviolet and visible spectrophotometer (Shimadzu Corporation, Japan) and a Hitachi F-4600 fluorescence spectrophotometer. A PHS-3C pH meter (INESA instruments) was used to measuring pH. Cell imaging was performed on Nikon A1 plus confocal microscope (Nikon, Japan). TLC analysis and column chromatography were carried out by using silica gel plates and silica gel (mesh 200-300) columns (Yantai Jiangyou Silica Gel Development Company Limited). The average sizes of polymer dots were measured by dynamic light scattering (DLS) (Malvern Zetasizer Nano ZS90) at room temperature. Transmission electron microscope images (TEM) were recorded on a field-emission high-resolution 2100F transmission electron microscope (JEOL, Japan).

DFT calculations. The ground state structure of compounds **RhCHO1**, **RhIndo2**, **RhBThia3**, **RhCN4**, **RhCOOEt5**, **RhPhCO6** and **RhAceton7** were optimized using DFT with B3LYP functional and 6-31G basis set, and using a CPCM solvation model (water). All of these calculations were performed with Gaussian 09 program package.[1]

Preparation of nano-probes. Polymer (mPEG-DSPE or mPEG-PPG-PEG) 4 mg and Np-RhPhCO (20.8 μM) were dissloved in 0.5 mL THF, then slowly poured into a vial containing 10 mL distilled-deionized water under vigorous sonication for 15 min. Then the THF of the mixed solution was removed by evaporation, and the residual solution was filtered. Finally, the initial nano-probes solution were obtained through further dialysis.

Spectra Studies and generation of RSS. For photophysical properties, the compounds **RhCHO1**, **RhIndo2**, **RhBThia3**, **RhCN4**, **RhCOOEt5**, **RhPhCO6**, **RhAceton7** and **Np-RhPhCO** were dissolved in CH_3CN to make the final stock solutions (500 μM). Sources for different RSS/ROS/RNS are described as following. Na_2SO_4, Na_2SO_3, $Na_2S_2O_3$, $NaHSO_3$, NaSCN and $NaNO_2$ were dissolved in distilled water. Specifically, H_2S, H_2S_2 and H_2S_4 were generated from that Na_2S, Na_2S_2 and Na_2S_4 were dissolved in distilled water, respectively. S_8 were dissolved in DMSO. Superoxide ($O_2^{\bullet-}$) was generated from KO_2 was dissolved in

DMSO. H_2O_2 (Sigma-Aldrich) and NaOCl (commercial bleach) were added into the testing solution directly for required concentration. GSSH and CysSSH were generated *in situ* from GSH and Cys, respectively, by the reaction with Na_2S and NO donor (NOC7) GSSH (NOC7 (50 μM) + Na_2S (50 μM) + GSH (50 μM)), CysSSH (NOC7 (50 μM) + Na_2S (50 μM) + Cys (50 μM)).[2] Probe and related persulfide precursors were mixed well prior to measurement, thereby allowing the reaction between probe and freshly produced CysSSH and GSSH.

Cell culture and Cell cytotoxicity study. HL-7702 and RAW 264.7 were cells cultured at 37 °C and 5% CO_2, using high glucose Dulbecco's Modified Eagle Medium (Hyclone) mixed with 10% fetal bovine serum (Gemini) and 1% antibiotics (100 U/mL penicillin and 100 μg/mL streptomycin, Hyclone). Cells were cultured in 96-well flat-bottomed plates for 24 h, and incubated nano-probe **PPG-Np-RhPhCO**. Subsequent operations were based on standard MTT assay. Finally, the absorbance was measured at 490 nm by a multidetection microplate reader. The following formula was used to calculate the viability of cell growth: Cell viability (%) = (mean of A value of treatment group - mean of A value of control) × 100.

Fluorescence microscopic imaging and image analysis. Fluorescence imaging of **PPG-Np-RhPhCO**, MITO-CC and TPC-N_3 in live cells. RAW 264.7 and HL-7702 cells were plated with 1.0 ml of DMEM (10% FBS and 1% antibiotics) in a 35-mm glass bottom dish and kept for 24 h at 37 °C. Seeded density of cells were 60%. And cells were incubated nano-probe **PPG-Np-RhPhCO** (40 μg/mL, 4.8 μM, 2 h), MITO-CC (5 μM, 30 min) and TPC-N_3 (5 μM, 30 min) respectively, then washed prior to imaging. The confocal imaging was performed using Nikon A1 plus confocal microscope with a 40 × water objective. All live images were acquired with an environment chamber at 37 °C. The fluorescence images of **PPG-Np-RhPhCO** were captured from the green channel of 425-475 nm and red channel of 570-620 nm with an excitation at 405 nm. The fluorescence imaging of MITO-CC were performed with acquiring the green channel (425-475 nm) and red channel (660-730 nm) with an excitation at 405 nm. The fluorescence images of TPC-N_3 were captured from the green channel (500-550 nm) with an excitation at 405 nm. Images were acquired at 16-bit depth with Nikon Elements Software and processed in Image J2 software by calculating its average values. Ratio images were constructed by image pro plus 6.0 software. Three replicates were performed for each imaging experiment.

FFA-induced NAFLD cell model. To establish a cellular model of NAFLD, the L02 cells were treated for 12 h with 0.5 mM FFA including the mixture of oleate and palmitate in a ratio of 2:1. And the L02 cells were treated 0.5 mM FFA for 12 h and washed with DPBS,

then treated with 3 mM acetaminophen (APAP) for 12 h to construct a drug-added NAFLD cell model.

Two-photon microscopic imaging studies. L02 cells were incubated nano-probe **PPG-Np-RhPhCO** (40 μg/mL, 4.8 μM) for 2 h then washed prior to imaging. The 3-7 days old zebrafishes (Eze-Rinka Company, China) were cultured in 5 mL of embryo medium mixed with 1-phenyl-2-thiourea (PTU) in 6-well plates for 24 h at 30 ℃. Zebrafishes were incubated with 14.4 μM **PPG-Np-RhPhCO** for 2 h at 30 ℃ then washed prior to imaging. Slices were prepared from the fresh liver of female KM mice (18-20 g). Slices were cut to 400 μm thickness by using a vibrating-blade microtome in 25 mM PBS (pH 7.4). And slices were incubated with 14.4 μM **PPG-Np-RhPhCO** for 4 h at 37 ℃ then washed prior to imaging. The two-photon confocal imaging was performed using Nikon A1 plus confocal microscope with a 10 × or 40 × water objective. The two-photon fluorescence emission was collected at 425-475 nm and 570-620 nm with excitation wavelength at 820 nm. All animal procedures were performed in accordance with the Guidelines for Care and Use of Laboratory Animals of Hunan University, and all animal experiments were approved by the Animal Ethics Committee of College of Biology (Hunan University).

Two-photon tissues imaging in NAFLD animal model. NAFLD animal model was built *via* high fat diet (HFD)-fed mice according to the reported studies.[3] Female KM mice aged 5 weeks were fed for 8 weeks with one of the following diets: (1) the common mice feed (a control diet); (2) a high fat diet containing 68.8 % the common mice feed, 20 % lard, 10 % Egg yolk powder, 0.2 % sodium cholate and 1 % cholesterol (HFD). Each group had ten mice that were given free access to food and water throughout the study. After 8 weeks, mice were treated with APAP or saline after an overnight fast. APAP was dissolved in warm saline and injected intraperitoneally at the dose of 300 mg/kg body weight, whereas saline was administered to control animals. After 6h, mice were sacrificed, and livers tissues were taken out and prepared as tissue imaging samples. Then, liver slices were incubated with 14.4 μM PPG-Np-RhPhCO in 25 mM PBS (pH 7.4) for 4 h at 37 ℃ then washed prior to the two-photon confocal imaging.

Western bolt. HL-7702 cells were lysed with RIPA Lysis Buffer (150 mM NaCl, 1% NP-40, 0.1% SDS, 50 mM Tris-HCl, pH 7.4). Total protein was isolated according to standard procedures and quantified using nanodrop. The proteins were separated by 10% sodium dodecyl sulfate polyacrylamide gel electrophoresis (SDS-PAGE) and then transferred onto nitrocellulose membrane using standard protocol. To block nonspecific antibody binding, the membrane was treated with 5% nonfat milk (dissolved in TBST) for 1.5 h. Next, the membrane was incubated with antibodies for Mercaptopyruvate Sulfurtransferase (MPST,

1:100, Santa cat. no. sc-374326) or Gamma Cystathionase (CSE, 1:1000, Proteintech cat. no.12217-1-AP) or β-actin (1:5000, Proteintech cat. no. 60008-1-Ig). The membranes were washed and incubated with HRP-conjugated goat anti-rabbit IgG (1:5000, Proteintech), then washed, and finally visualized using a chemiluminescence (ECL) system.

Oil Red O (ORO) staining experiments. L02 cells were cultured on chamber slide (Corning Life Sciences, Acton, MA, USA; 3650) in per well for 24 h, and then incubated with the indicated treatments. After being fixed for 60 min at 25 °C by 4% paraformaldehyde (PFA), culture medium was discarded and cells were rinsed three times with DPBS. Next, the cells were stained with 0.5% Oil Red O (ORO) solution for 5 min and then with hematoxylin solution (Sigma-Aldrich) for 1 min. Finally, slides were washed to microscopy analysis. To quantify the cellular content of ORO, L02 cells were firstly incubated with 100 μL isopropanol for 10 min, then extracted to assess their absorbance at 490 nm with a multi-functional enzyme label analyzer (MB-530, Shenzhen Huisong, China).

Measurement of cellular triglyceride (TG) in L02 cells. Intracellular triglyceride (TG) contents of L02 cells were assayed using commercial kits purchased from Nanjing Jiancheng Bioengineering Institute (Nanjing, China) according to the manufacturer's recommended protocols. The protein concentration in the resulting lysates was determined using the BCA (bicinchonininc acid) protein assay kit (Sigma-Aldrich).

2. The structure of seven compounds

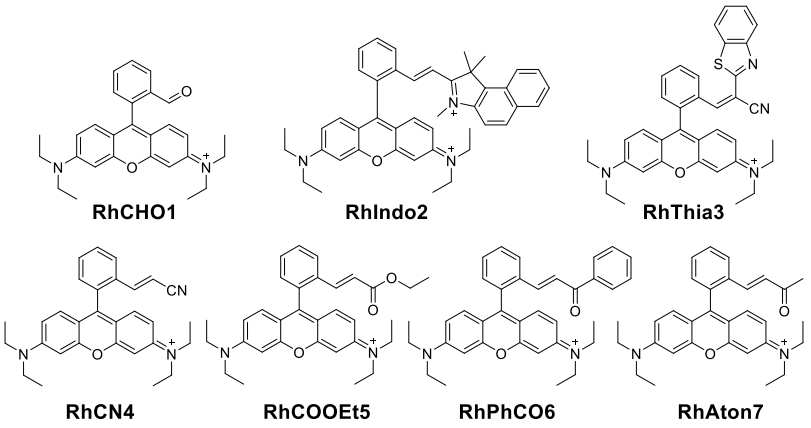

Scheme S1. The structure of compounds **RhCHO1**, **RhIndo2**, **RhBThia3**, **RhCN4**, **RhCOOEt5**, **RhPhCO6**, **RhAceton7**.

3. The synthesis and characterization of seven compounds

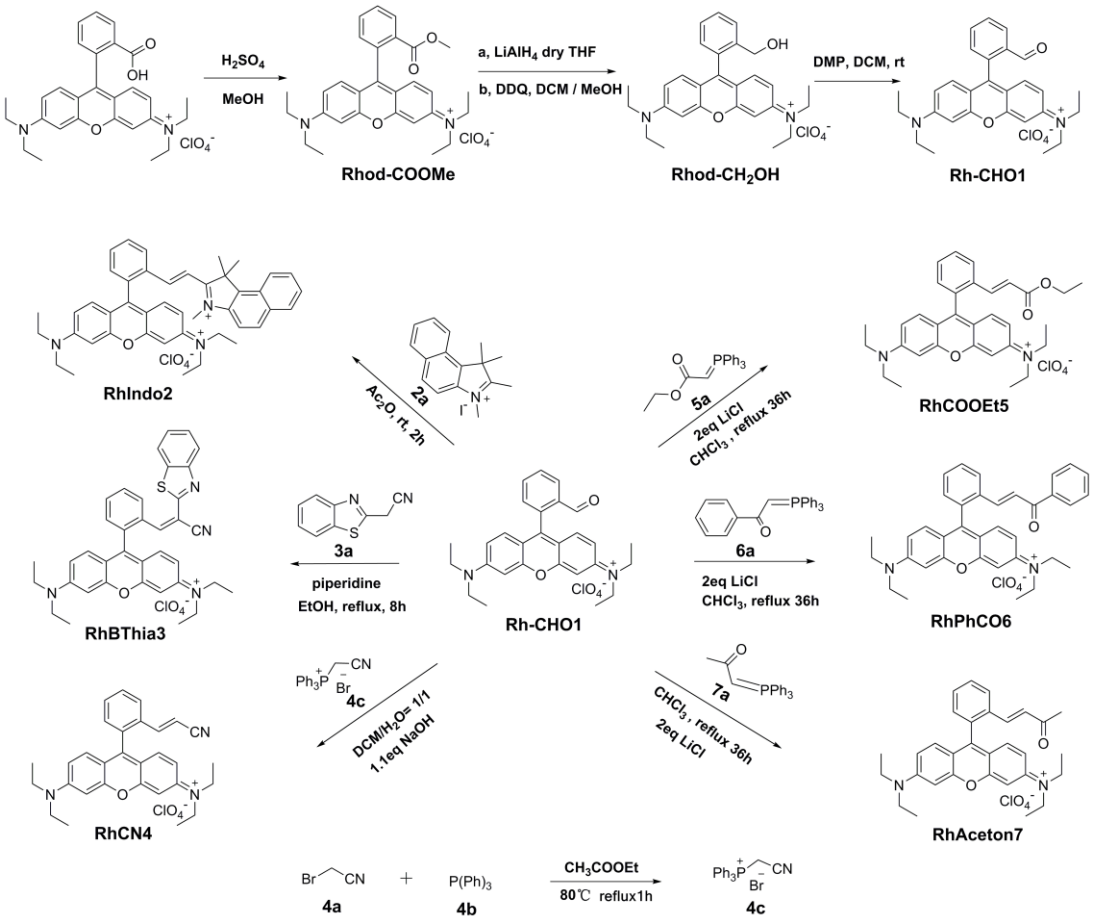

Scheme S2. Synthetic routes of compounds **RhCHO1**, **RhIndo2**, **RhBThia3**, **RhCN4**, **RhCOOEt5**, **RhPhCO6**, **RhAceton7**.

Synthesis of Compound Rhod-COOMe

Rhodamine B (960.2 mg, 2 mmol) was dissolved in 20 mL MeOH. The concentrated H_2SO_4 (8 mL) was added dropwise to the solution and cooled down to 0 °C, and then stirred overnight at 80 °C. When the mixture was cooled to room temperature, the solvent was removed by evaporation, and the residue was poured onto ice, perchloric acid (70%, 2 mL) was then added, and the resulting precipitate was filtered off and the filtrate was dissolved in CH_2Cl_2 and the solution was washed with water and saturated $NaHCO_3$. The organic layer was dried over Na_2SO_4 and evaporated to dryness. The resulting precipitate and the residue was purified by silica gel column chromatography (CH_2Cl_2/MeOH = 25/1) to afford compound **Rhod-COOMe** (830.4 mg, 74.6% yield) as red solid. ^{1}H NMR (400 MHz, $CDCl_3$) δ 8.29 (d, J = 7.9 Hz, 1H), 7.82 (t, J = 7.4 Hz, 1H), 7.74 (t, J = 7.5 Hz, 1H), 7.32 (d, J = 7.5 Hz, 1H), 7.06 (d, J = 9.1 Hz, 2H), 6.86 (s, 3H), 6.84 (s, 1H), 3.68 (s, 3H), 3.62 (q, J = 7.0 Hz, 8H), 1.33 (t, J = 6.9 Hz, 12H). ^{13}C NMR (100 MHz, $CDCl_3$) δ 166.7, 160.3, 159.6, 157.8, 155.5, 148.4, 133.1, 131.2, 131.2, 130.3, 114.1, 113.5, 99.9, 96.5, 52.6, 46.0, 12.6.

Synthesis of Compound Rhod-CH_2OH

The **Rhod-COOMe** (300.8 mg, 0.54 mmol) was dissolved and decentralized in dry THF at 0 °C, and then a solution of $LiAlH_4$ (164.9 mg, 4.3 mmol) in dry THF (10 mL) was slowly added to it. The mixture was brought to room temperature and stirred for 4 h. The reaction was stopped by addition of saturated NH_4Cl_4 (2 mL), and THF was removed by evaporation. The resulting residue was dissolved in CH_2Cl_2 and hot MeOH, then the resulting precipitate was filtered off and the filtrate was removed by evaporation to give a purple solid without purification. The crude intermediate was dissolved in 5 mL of CH_2Cl_2, and *p*-chloranil (DDQ) 153.5 mg (0.67 mmol, 1.2 eq) in 5 mL MeOH was then added. The reaction mixture was stirred for 1.5 h, the residue was purified by silica gel column chromatography (CH_2Cl_2/MeOH = 30/1) to afford compound **Rhod-CH_2OH (**80.6 mg, 28% yield) as red solid. ^{1}H NMR (400 MHz, $CDCl_3$) δ 7.68 (d, J = 7.1 Hz, 1H), 7.52 (t, J = 7.0 Hz, 1H), 7.38 (t, J = 6.9 Hz, 1H), 7.13 (d, J = 7.8 Hz, 2H), 7.07 (d, J = 5.5 Hz, 1H), 6.78 (d, J = 7.2 Hz, 2H), 6.71 (s, 2H), 4.41 (s, 2H), 3.53 (d, J = 3.5 Hz, 8H), 1.26 (d, J = 4.9 Hz, 12H).

Synthesis of Compound Rh-CHO1

To a solution of **Rhod-CH_2OH** (80.1 mg, 0.2 mmol) in 5 mL CH_2Cl_2, DMP (1,1,1-Triacetoxy - 1,1-Dihydro-1, 2-Benziodoxol-3(1H)-One**)** (80.7 mg, 0.25 mmol) were slowly added. The mixture was stirred at room temperature for 1 h. The organic layer was washed with $Na_2S_2O_3$ and brine. The organic layer was dried over Na_2SO_4 and evaporated to dryness. The residue was purified by silica gel column chromatography (CH_2Cl_2/MeOH = 40/1) to afford compound **RhCHO1** (60.6 mg, 73.3% yield) as red solid. ^{1}H NMR (400 MHz, $CDCl_3$) δ 9.85 (s, 1H), 9.29 – 9.11 (m, 1H), 8.19 (d, J = 7.2 Hz, 1H), 8.00 – 7.70 (m, 2H), 7.37 (d, J = 7.0 Hz, 1H), 7.02 (d, J = 9.4 Hz, 2H), 6.92 (d, J = 9.4 Hz, 2H), 6.80 (s, 2H), 3.63 (dd, J = 13.2, 6.3 Hz, 7H), 1.30 (t, J = 6.4 Hz, 12H). ^{13}C NMR (100 MHz, $CDCl_3$) δ 190.3, 157.6, 156.0, 155.6, 134.6, 132.9, 132.6, 131.1, 130.5, 114.6, 113.8, 96.4, 46.2, 12.6. MS (ESI) : m/z [M^+] = 427.2.

Synthesis of Compound RhIndo2

RhCHO1 (42.7 mg, 0.1 mmol) and compound **2a** (36.8 mg, 0.15 mmol) were dissolved in acetic anhydride (2 mL), and the mixture was stirred at room temperature for 2 h. After completion of the reaction and solvent removal under reduced pressure, the residues was purified by flash chromatography (DCM/EtOH = 100/1) to afford the product **RhIndo2** as a red solid (19.3 mg, 30.4% yield). ^{1}H NMR (400 MHz, $CDCl_3$) δ 9.86 (s, 1H), 8.20 (d, J = 7.4 Hz, 1H), 7.92 (t, J = 7.3 Hz, 1H), 7.87 (t, J = 7.6 Hz, 1H), 7.64 (d, J = 3.9 Hz, 1H), 7.43 (d, J = 7.4 Hz, 1H), 7.12 (d, J = 9.5 Hz, 2H), 7.05 (d, J = 9.5 Hz, 2H), 6.93 (t, J = 9.6 Hz, 3H), 6.85 (d, J = 6.4 Hz, 3H), 4.80 (s, 2H), 3.65 (dd, J = 15.2, 7.5 Hz, 12H), 1.81 (s, 3H), 1.33 (d, J = 3.4 Hz, 18H). ^{13}C NMR (100 MHz, $CDCl_3$) δ 189.2, 156.8, 156.6, 154.9, 154.7, 154.6, 133.6, 133.1, 132.0, 131.5, 130.6, 130.2, 130.0, 129.6, 129.4, 128.8, 128.6, 128.3, 127.9, 113.6, 113.4, 112.9, 112.7, 95.6, 95.5, 62.6, 45.4, 45.3, 28.6, 11.7.

Synthesis of Compound RhBThia3

RhCHO1 (42.6 mg, 0.1 mmol) and compound **3a** (34.8 mg, 0.2 mmol) were dissolved in EtOH (3 mL), and added piperidine (60 μL), The resulting mixture was refluxed for 8 h. After overnight reaction, the mixture was cooled to room temperature, and EtOH was removed under reduced pressure, and the residue was purified by silica gel column chromatography to afford the compound **RhBThia3** (13.1mg, 22.4% yield). ^{1}H NMR (400 MHz, $CDCl_3$) δ 8.45 (d, J = 7.9 Hz, 1H), 7.98 (d, J = 8.2 Hz, 1H), 7.84 (d, J = 8.2 Hz, 1H), 7.82 – 7.75 (m, 2H), 7.69 (s, 1 H), 7.48 – 7.42 (m, 2H), 7.41 (d, J = 7.8 Hz, 1H), 7.12 (d, J = 9.3 Hz, 2H), 7.05 (s, 2H), 6.86 (d, J = 11.5 Hz, 2H), 3.62 (dd, J = 13.4, 6.5 Hz, 8H), 1.32 (d, J = 6.3 Hz, 12H). HRMS (m/z): calcd for $C_{37}H_{35}N_4OS$ [M^+]: 583.2526, found: 583.2525.

Synthesis of Compound RhCN4

2-bromoacetonitrile (240.2 mg, 2 mmol) and PPh_3 (520.6 mg, 2 mmol) were dissolved in ethyl acetate (10 mL), the resulting mixture was heated to 80 °C for 1 h. After completion of the reaction, the resulting precipitate was filtered to get crude product **4c** (625.3 mg, 82.0% yield) as white solid. The white solid **4c** (45.2 mg, 0.15 mmol) and **RhCHO1** (42.7 mg, 0.1 mmol) were dissolved in 4 mL CH_2Cl_2, the mixture was stirred at room temperature for 30 min. Then NaOH (4.4 mg, 0.11 mmol) dissolved in 1 mL water was slowly added. The resulting reaction mixture was stirred at room temperature for overnight, and water (20 mL) was added. The layer were separated, and added 50 mL CH_2Cl_2 to extracted three times. The organic layer was dried over Na_2SO_4 and evaporated under reduced pressure, then the crude product was purified by silica gel column chromatography (CH_2Cl_2/MeOH = 80/1) to afford compound **RhCN4** (7.3 mg, 16.2% yield) as red solid. ^{1}H NMR (400 MHz, $CDCl_3$) δ 8.32 (d, J = 7.7 Hz, 1H), 7.91 (d, J = 3.3 Hz, 1H), 7.75 – 7.69 (m, 2H), 7.36 (d, J = 6.5 Hz, 1H), 7.09 (d, J = 9.9 Hz, 2H), 6.95 (d, J = 10.1 Hz, 2H), 6.90 (s, 2H), 6.04 (d, J = 16.4 Hz, 1H), 3.68 (s, 8H), 1.36 (d, J = 5.7 Hz, 12H). HRMS (m/z): calcd for $C_{30}H_{32}N_3O$ [M^+]: 450.2540, found: 450.2539.

Synthesis of Compound RhCOOEt5

RhCHO1 (21.9 mg, 0.04 mmol) and compound **5a** (40.6 mg, 0.1 mmol) were dissolved in 3 mL chloroform, and added LiCl (4.8 mg, 0.1 mmol). The resulting mixture was refluxed for 36 h. After completion of the reaction, the mixture was cooled to room temperature. $CHCl_3$ was removed under reduced pressure, and the residue was purified by silica gel column chromatography to afford the compound **RhCOOEt5** (9.9 mg, 42.3% yield). ^{1}H NMR (400 MHz, $CDCl_3$) δ 7.84 (d, J = 7.0 Hz, 1H), 7.59 (dd, J = 14.7, 7.1 Hz, 2H), 7.20 (s, 1H), 7.10 (d, J = 15.8 Hz, 1H), 7.01 (d, J = 9.1 Hz, 2H), 6.87 (d, J = 9.2 Hz, 2H), 6.78 (s, 2H), 6.41 (d, J = 15.8 Hz, 1H), 4.06 (dd, J = 13.1, 6.3 Hz, 2H), 3.61 (d, J = 6.2 Hz, 8H), 1.27 (s, 12H), 0.81 (s, 3H). ^{13}C NMR (100 MHz, $CDCl_3$) δ 166.3, 157.8, 155.8, 155.1, 140.1, 135.8, 133.3, 132.4, 132.3, 131.7, 130.7, 130.5, 130.1, 126.8, 121.5, 114.7, 113.9, 96.6, 60.8, 46.4, 14.2, 12.8. HRMS (m/z): calcd for $C_{32}H_{37}N_2O_3$ [M^+]: 497.2799, found: 497.2798.

Synthesis of Compound RhPhCO6

RhCHO1 (42.6 mg, 0.1 mmol) and compound **6a** (76.1 mg, 0.2 mmol) were dissolved in 3 mL chloroform, and added LiCl (8.4 mg, 0.2 mmol), The resulting mixture was refluxed for 36 h. After completion of the reaction, the mixture was cooled to room temperature. $CHCl_3$ was removed under reduced pressure, and the residue was purified by silica gel column chromatography to afford the compound **RhPhCO6** (15.5 mg, 29.3% yield). ^{1}H NMR (400 MHz, $CDCl_3$) δ 8.02 (d, J = 7.2 Hz, 1H), 7.82 (d, J = 7.2 Hz, 2H), 7.70 - 7.63 (m, 1H), 7.61 (d, J = 7.0 Hz, 1H), 7.54 (d, J = 15.9 Hz, 1H), 7.49 (d, J = 7.6 Hz, 1H), 7.38 (t, J = 7.1 Hz, 2H), 7.25 (d, J = 8.6 Hz, 1H), 7.21 (s, 1H), 7.06 (d, J = 8.9 Hz, 2H), 6.86 (d, J = 8.9 Hz, 2H), 6.78 (s, 2H), 3.59 (d, J = 6.2 Hz, 8H), 1.26 (s, 12H). ^{13}C NMR (100 MHz, $CDCl_3$) δ 189.6, 157.9, 155.9, 155.5, 140.1, 137.5, 133.9, 133.4, 132.9, 131.8, 130.9, 130.8, 130.2, 128.8, 128.6, 127.1, 124.9, 114.8, 114.0, 96.7, 46.4, 12.8. HRMS (m/z): calcd for $C_{36}H_{37}N_2O_2$ [M^+]: 529.2850, found: 529.2850.

Synthesis of Compound RhAceton7

RhCHO1 (22.7 mg, 0.04 mmol) and compound **7a** (37.1 mg, 0.1 mmol) were dissolved in 3 mL chloroform, and added LiCl (5.4 mg, 0.1 mmol). The resulting mixture was refluxed for 36 h. After completion of the reaction, the mixture was cooled to room temperature. $CHCl_3$ was removed under reduced pressure, and the residue was purified by silica gel column chromatography to afford the compound **RhAceton7** (8.9 mg, 38.3% yield). ^{1}H NMR (400 MHz, $CDCl_3$) δ 7.87 (d, J = 7.7 Hz, 1H), 7.59 - 7.55 (m, 2H), 7.53 (d, J = 5.6 Hz, 1H), 7.44 (d, J = 7.1 Hz, 1H), 7.37 (d, J = 7.0 Hz, 1H), 7.17 (d, J = 7.0 Hz, 1H), 6.99 (d, J = 9.4 Hz, 1H), 6.94 (d, J = 16.0 Hz, 1H), 6.80 (d, J = 9.7 Hz, 1H), 6.77 (s, 1H), 6.71 (d, J = 15.9 Hz, 1H), 3.55 (q, J = 6.8 Hz, 8H), 2.08 (s, 3H), 1.22 (t, J = 6.8 Hz, 12H). ^{13}C NMR (100 MHz, $CDCl_3$) δ 197.5, 157.4, 155.4, 154.7, 138.0, 133.1, 132.5, 132.3, 131.8, 131.8, 131.7, 131.6, 131.3, 130.5, 130.2, 129.8, 129.0, 128.3, 128.2, 126.8, 114.3, 113.4, 96.3, 45.9, 28.5, 12.3. HRMS (m/z): calcd for $C_{31}H_{35}N_2O_2$ [M^+]: 467.2693, found: 467.2692.

4. The synthesis and characterization of probe Np-RhPhCO

Synthesis of 4-bromo-2-formylbenzoic acid

4-bromo-2-formylbenzoic acid was synthesized as previously described.[4]

Synthesis of Compound Br-Rhod-COOH

The compound 4-bromo-2-formylbenzoic acid (1145.3 mg, 5 mmol), p-methylphenyl sulphonylamine (171.2 mg, 1 mmol) and m-diethylphenol (2062.9 mg, 2.5 mmol) were dissolved in 8 mL of propanoic acid. The resulting mixture was refluxed for 5 h. After completion of the reaction, the mixture was cooled to room temperature. And the residue was poured onto ice water, perchloric acid (70%, 8 mL) was then added, and was placed in the refrigerator for 3 hours. the resulting precipitate was filtered off. The resulting precipitate was purified by silica gel column chromatography (CH_2Cl_2/MeOH = 30/1) to afford compound **Br-Rhod-COOH** (1560.6 mg,

59.8% yield) as red solid. ^{1}H NMR (400 MHz, $CDCl_3$) δ 8.10 (d, J = 8.5 Hz, 1H), 7.70 (dd, J = 8.5, 1.6 Hz, 1H), 7.31 (d, J = 1.6 Hz, 1H), 7.04 (d, J = 9.4 Hz, 2H), 6.77 (dd, J = 9.5, 1.9 Hz, 2H), 6.72 (d, J = 1.8 Hz, 2H), 3.56 (q, J = 6.9 Hz, 8H), 1.26 (t, J = 7.0 Hz, 12H). ^{13}C NMR (100 MHz, $CDCl_3$) δ 165.9, 156.6, 154.3, 134.5, 132.1, 132.0, 131.2, 131.0, 130.3, 125.3, 112.9, 112.3, 95.2, 45.0, 11.6. MS (ESI): m/z [M^+] = 521.1.

Synthesis of Compound Br-Rhod-CH_2OH

The compound **Br-Rhod-COOH** (880.1 mg, 2 mmol) was dissolved in 20 mL MeOH. 4 mL concentrated H_2SO_4 was added dropwise to the solution at 0 °C, and then stirred overnight at 80 °C. When the mixture was cooled to room temperature, the solvent was removed by evaporation, and the residue was poured onto ice, perchloric acid (70%, 2 mL) was then added and placed in the refrigerator for 5 h, and the resulting precipitate was filtered off to give a red solid without purification. The red solid (792.4 mg, 1.25 mmol) was dissolved and decentralized in dry THF at 0 °C, and then a solution of $LiAlH_4$ (360.3 mg, 9.4 mmol) in dry THF 10 mL was slowly added to it. The mixture was brought to room temperature and stirred for 4 h. The reaction was stopped by addition of sat. NH_4Cl (4 mL), and THF was removed by evaporation. The resulting residue was dissolved in CH_2Cl_2 and hot MeOH, then filtered through a short plug of silica. Removal of the solvent gave a crude mixture which was purified by column chromatography (hexane/acetone = 1/3). and the resulting precipitate was filtered off and the filtrate was removed by evaporation to give a purple solid without purification. The crude intermediate was dissolved in 6 mL of CH_2Cl_2, and DDQ (*p*-chloranil) (324.6 mg, 1.32 mmol) in 6 mL of MeOH was then added. The reaction mixture was stirred for 1.5 h, the residue was purified by silica gel column chromatography (CH_2Cl_2/MeOH = 30/1) to afford compound **Br-Rhod-CH_2OH** (235.4 mg, 31.0%) as red solid. ^{1}H NMR (400 MHz, $CDCl_3$) δ 7.62 (s, 2H), 7.20 (s, 1H), 7.11 (d, J = 9.3 Hz, 2H), 6.82 (d, J = 9.4 Hz, 2H), 6.72 (s, 2H), 4.29 (s, 2H), 3.54 (d, J = 5.0 Hz, 8H), 1.25 (t, J = 6.6 Hz, 12H). ^{13}C NMR (100 MHz, $CDCl_3$) δ 156.8, 154.7, 153.9, 138.3, 132.2, 131.0, 130.7, 130.0, 129.3, 120.0, 113.5, 112.4, 95.4, 60.6, 45.1, 11.6. MS (ESI): m/z [M^+] = 507.2.

Synthesis of Compound Br-Rhod-CHO

To a solution of **Br-Rhod-CH_2OH** (235.4 mg) in 5 mL CH_2Cl_2, DMP (1,1,1-Triacetoxy-1,1-Dihydro-1, 2-Benziodoxol-3(1H)-One, 240.8 mg) was slowly added. The mixture was stirred at room temperature for 1 h. The organic layer was washed with $Na_2S_2O_3$ and brine. And the organic layer was dried over Na_2SO_4 and evaporated to dryness. The residue was purified by silica gel column chromatography (CH_2Cl_2/MeOH = 40/1) to afford compound **Br-Rhod-CHO** (188.6 mg, 81.9%) as red solid. ^{1}H NMR (400 MHz, $CDCl_3$) δ 9.78 (s, 1H), 8.08 (d, J = 8.4 Hz, 1H), 7.97 (d, J = 8.3 Hz, 1H), 7.49 (s, 1H), 7.03 (d, J = 9.3 Hz, 2H), 6.88 (d, J = 9.5 Hz, 2H), 6.84 (s, 2H), 3.65 – 3.58 (m, 8H), 1.30 (t, J = 6.1 Hz, 12H). ^{13}C NMR (100 MHz, $CDCl_3$) δ 189.5, 157.6, 155.8, 153.5, 134.7, 134.3, 133.8, 133.6, 133.2, 130.9, 129.7, 114.7, 113.6, 96.7, 46.2, 12.6. MS (ESI): m/z [M^+] = 505.1.

Synthesis of Compound Br-RhPhCO

Br-Rhod-CHO (170.4 mg, 0.4 mmol) and compound **6a** (304.4 mg, 0.8 mmol) were dissolved in 12 mL chloroform, and added LiCl (41.5 mg, 0.8 mmol), The resulting mixture was refluxed for 36 h. After completion of the reaction, the mixture was cooled to room temperature. $CHCl_3$ was removed under reduced pressure, and the residue was purified by silica gel column chromatography to afford the compound **Br-RhPhCO** (85.2 mg, 30% yield). ^{1}H NMR (400 MHz, MeOD) δ 8.31 (d, J = 7.9 Hz, 1H), 7.88 (d, J = 7.7 Hz, 2H), 7.81 (t, J = 7.6 Hz, 1H), 7.77 (s, 1H), 7.74 (d, J = 5.8 Hz, 1H), 7.67 (dd, J = 11.0, 6.0 Hz, 1H), 7.59 (d, J = 7.3 Hz, 2H), 7.46 (t, J = 6.3 Hz, 3H), 7.33 – 7.25 (m, 1H), 7.19 (d, J = 9.5 Hz, 2H), 7.09 (d, J = 10.6 Hz, 2H), 7.04 (s, 2H), 3.71 (q, J = 6.9 Hz, 8H), 1.34 (d, J = 6.8 Hz, 12H). ^{13}C NMR (100 MHz, MeOD) δ 190.6, 157.9, 155.9, 155.2, 140.5, 137.3, 133.8, 133.2, 133.0, 131.7, 131.6, 131.3, 130.5, 130.4, 129.9, 128.6, 128.5, 128.4, 128.2, 127.0, 124.7, 114.5, 113.7, 96.1, 45.5, 11.4. MS (ESI): m/z [M^+] = 607.1.

Synthesis of Compound Np-Borate

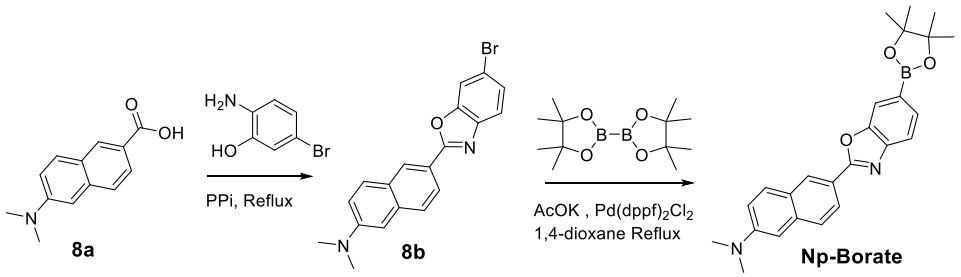

Scheme S3. Synthetic routes of compound **Np-Borate.**

Np-Borate was synthesized as previously described.[5]

Synthesis of Compound Np-RhPhCO

Br-RhPhCO (85.2 mg, 0.12 mmol), compound **Np-Borate** (149.3 mg, 0.36 mmol), $Pd(dppf)_2Cl_2$ (0.02 mmol, 20.3 mg) of and K_3PO_4 (103.9 mg, 0.48 mmol) were dissolved in 1,4-dioxane and H_2O (v/v, 10/1) under nitrogen, upon the temperature reached 80 ºC and refluxed 24 h after completion of the reaction by TLC, evaporated the solvent, the crude product was purified by column chromatography with (CH_2Cl_2/CH_3OH = 500/6) and afforded the target product **Np-RhPhCO** (26.3 mg, 23.1% yield). ^{1}H NMR (400 MHz, $CDCl_3$) δ 8.59 (s, 1H), 8.22 (d, J = 8.3 Hz, 1H), 8.14 (d, J = 8.6 Hz, 1H), 8.00 (d, J = 8.3 Hz, 1H), 7.91 (d, J = 7.9 Hz, 2H), 7.87 (s, 1H), 7.80 (t, J = 8.4 Hz, 2H), 7.74 – 7.67 (m, 2H), 7.65 (s, 1H), 7.59 (s, 1H), 7.56 (d, J = 7.2 Hz, 1H), 7.45 (t, J = 7.4 Hz, 3H), 7.32 (d, J = 15.4 Hz, 1H), 7.23 (d, J = 9.5 Hz, 2H), 6.95 (dd, J = 9.6, 1.8 Hz, 2H), 6.87 (s, 3H), 3.65 (d, J = 6.7 Hz, 8H), 3.10 (s, 6H), 1.32 (d, J = 6.8 Hz, 12H). ^{13}C NMR (100 MHz, $CDCl_3$) δ 189.6, 165.3, 157.9, 155.9, 155.1, 151.6, 150.0, 143.2, 139.6, 137.5, 137.0, 135.5, 133.8, 133.4, 132.8, 131.8, 130.2, 129.4, 128.8, 128.6, 128.5, 127.9, 126.8, 125.8, 124.6, 124.4, 124.0, 120.0, 119.6, 116.7, 114.9, 114.1, 109.1, 105.6, 96.8, 46.4, 29.8, 12.8. HRMS (m/z): calcd for $C_{55}H_{51}N_4O_3$ [M^+]: 815.3956, found: 815.3956.

5. The selectivity of seven compounds in fluorescence spectra

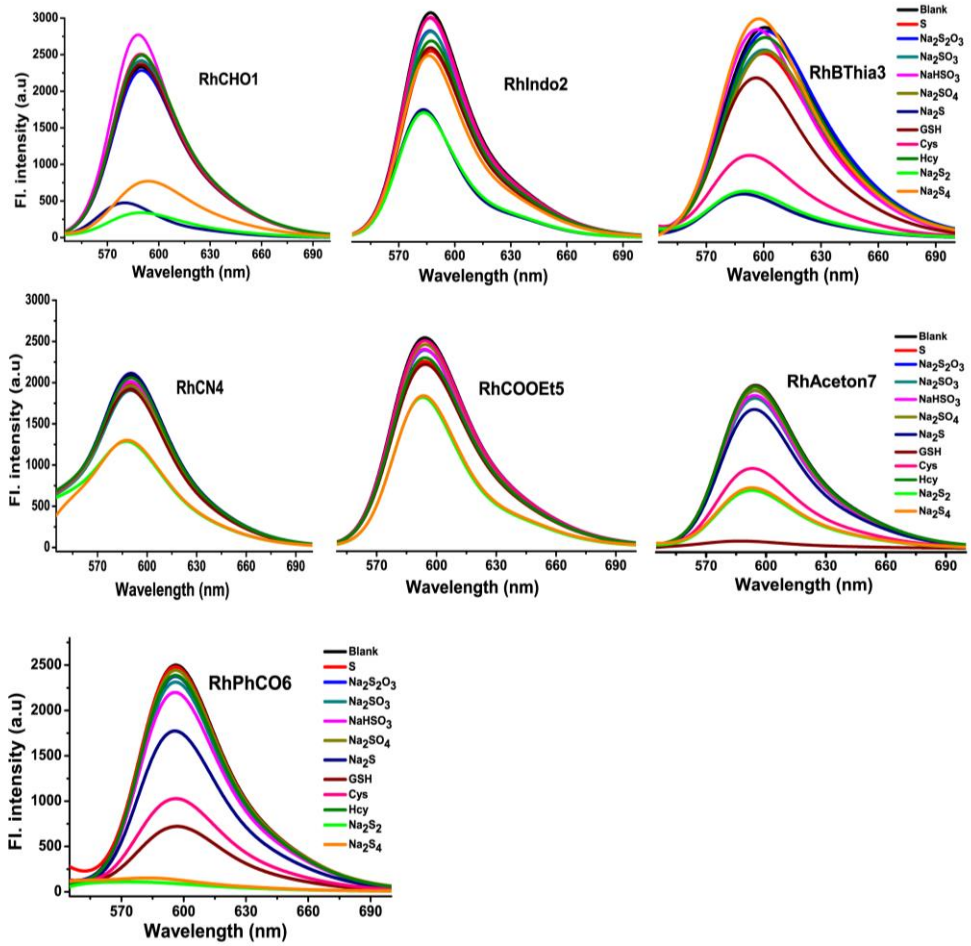

Fig. S1. Fluorescence changes of 5 μM of compounds **RhCHO1**, **RhIndo2**, **RhBThia3**, **RhCN4**, **RhCOOEt5**, **RhPhCO6**, and **RhAceton7** in the presence of 50 μM Na_2S_2 and other biologically relevant analytes in PBS (pH 7.4) at 37 °C. The mixture was kept for 30 min at a 37 °C shaker before measured. Data shown are for 1 mM glutathione, 50 μM Na_2S_4, and 200 μM for other analytes. λ_{ex} = 520 nm.

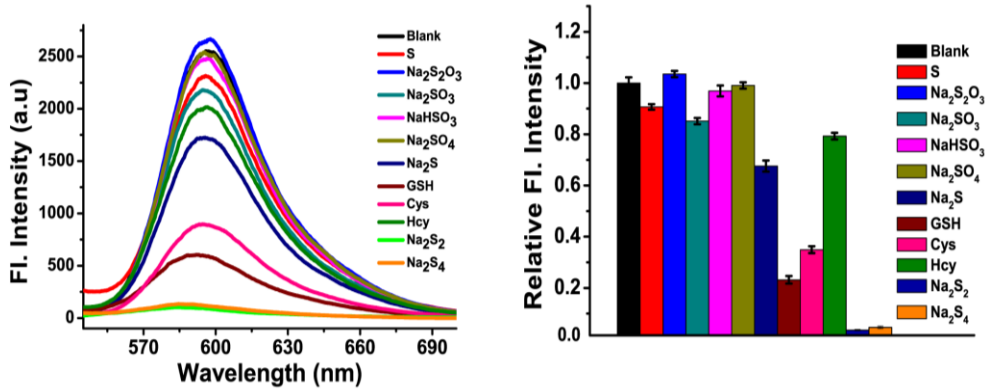

Fig. S2. Fluorescence changes of **RhPhCO6** (5 μM) in the presence of 50 μM Na_2S_2 and other RSS (5 mM glutathione, 50 μM Na_2S_4, and 200 μM for other analytes) in PBS (pH 7.4)

buffer at 37 °C. The mixture was kept for 2.5 h in a 37 °C shaker before measured. Bars represent the relative fluorescence intensity of 596 nm after addition of analytes. λ_{ex} = 520 nm.

6. Time-/pH-fluorescence intensity changes of RhPhCO6 upon addition 50 μM Na_2S_2

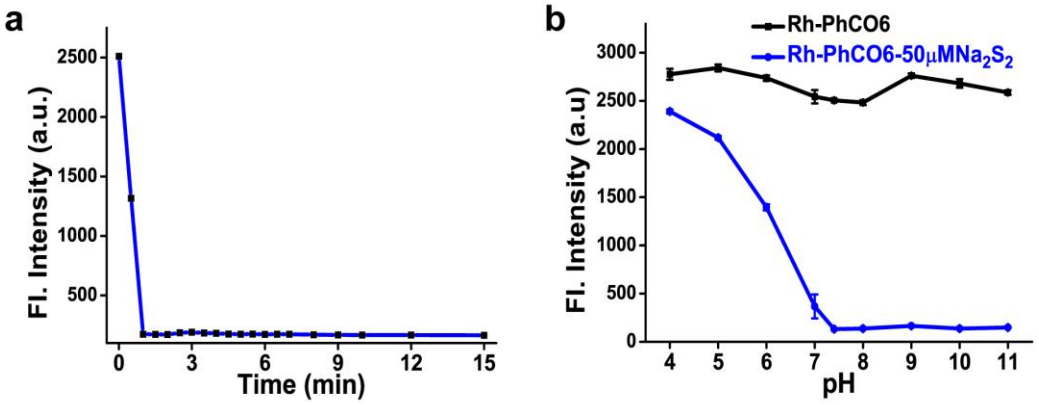

Fig. S3. (a) Time-fluorescence intensity changes of **RhPhCO6** (5 μM) upon addition 50 μM Na_2S_2 from 0 to 15 min. (b) pH-dependent fluorescence intensity changes of **RhPhCO6** toward 50 μM Na_2S_2 in PBS buffer (25 mM, pH = 4.0-11.0), $\lambda_{ex}/\lambda_{em}$ = 520/596 nm.

7. The DFT calculation results of seven compounds

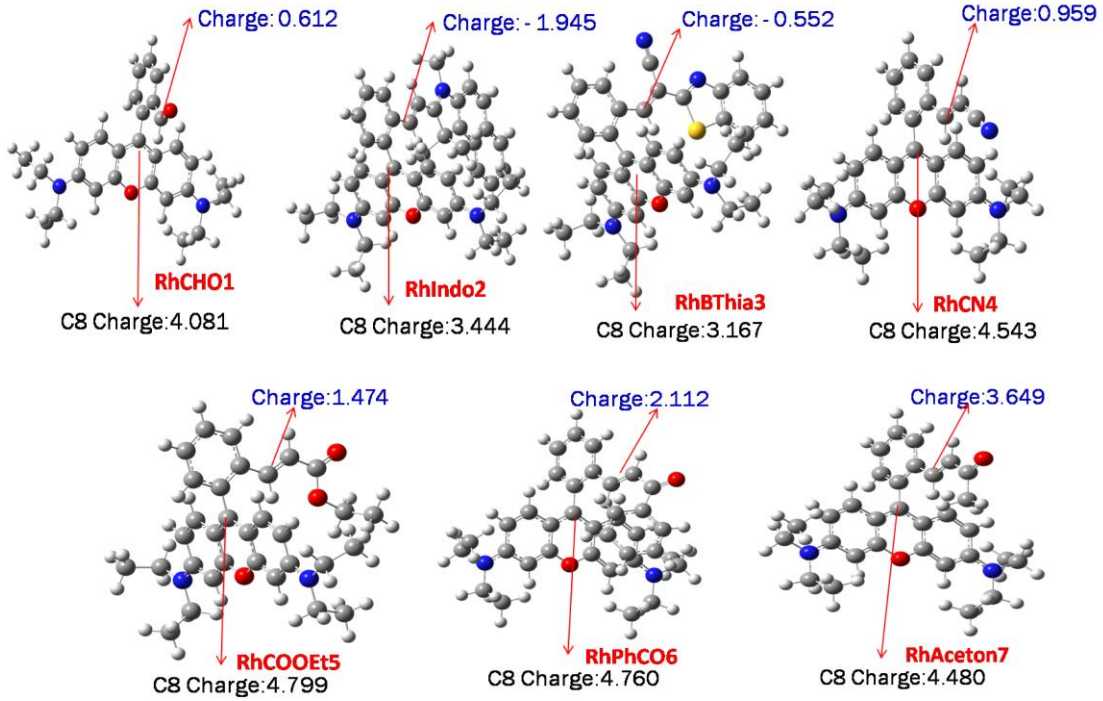

Fig. S4. Chemical structures of compounds **RhCHO1**, **RhIndo2**, **RhBThia3**, **RhCN4**, **RhCOOEt5**, **RhPhCO6**, and **RhAceton7**. And calculated electrostatic charges of the enone *β* carbons C_1 = C-CO (eV) and C_8 Charge (eV) of these compounds.

8. The proposed reaction mechanism of RhPhCO6 and Na_2S_2 with MS and ^1H NMR spectra

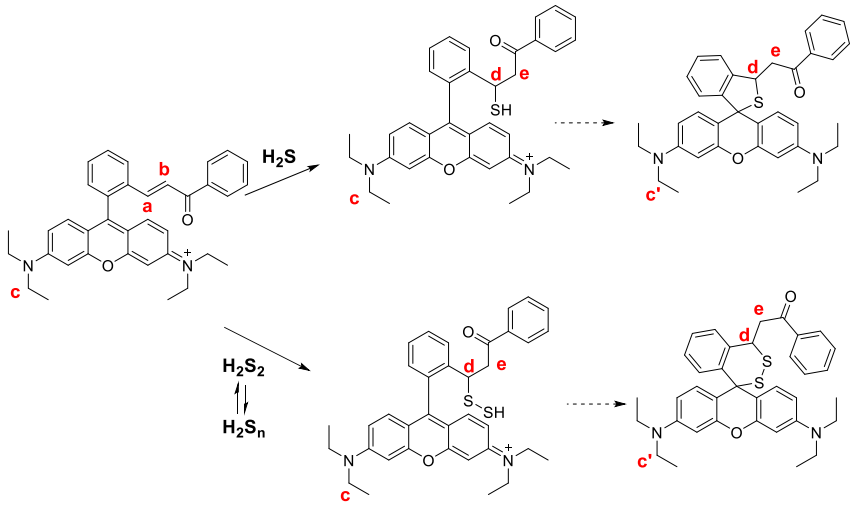

Fig. S5. The proposed reaction mechanism of **RhPhCO6** towards H_2S_2 and H_2S.

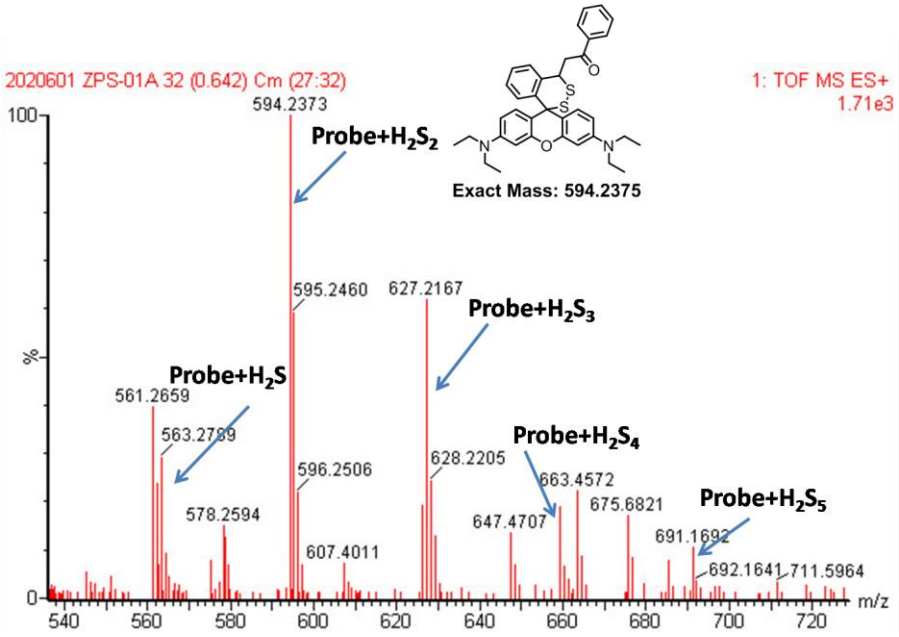

Fig. S6. The HR mass spectrum of probe RhPhCO6 in the presence of 1 equiv Na_2S_2.

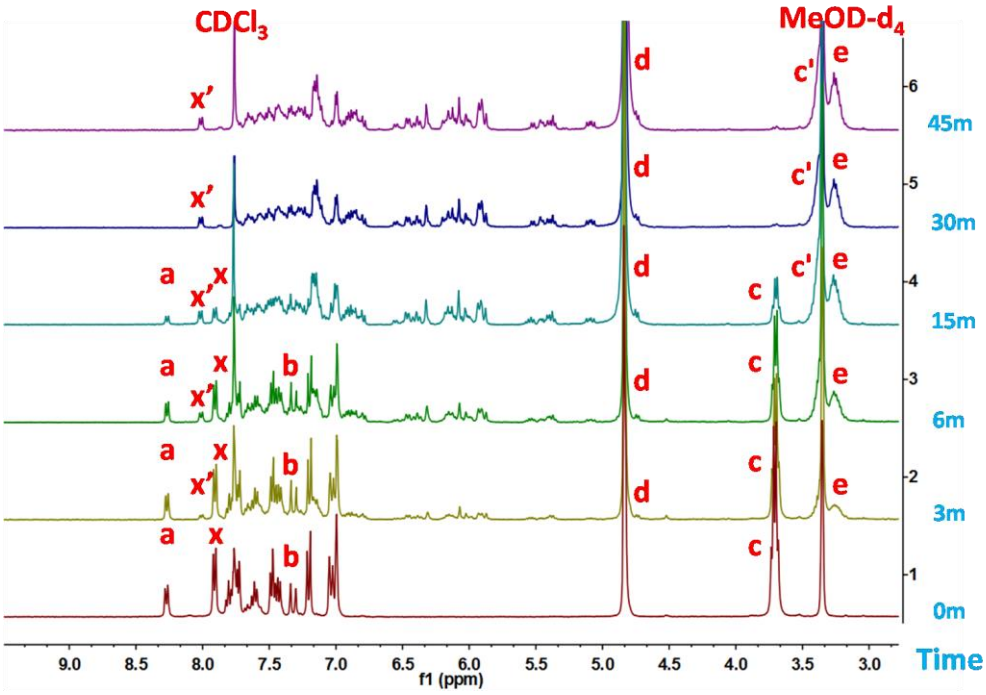

Fig. S7. Partial ^{1}H NMR spectra of probe RhPhCO6 with 1 equiv Na_2S_2 as a function of time in MeOD-d_4/$CDCl_3$ (2:1, v/v).

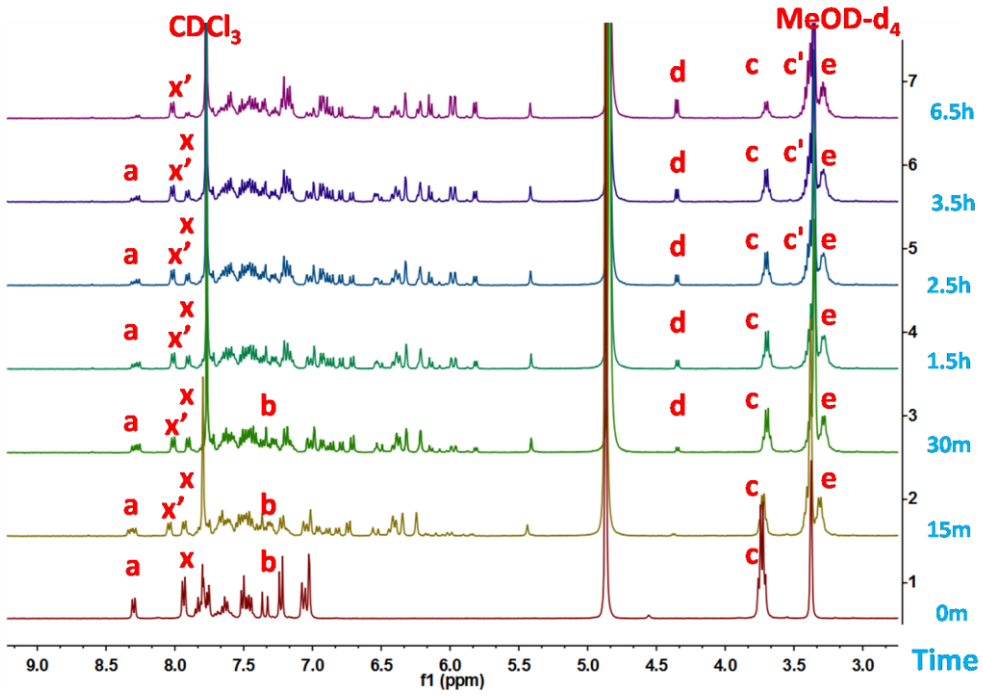

Fig. S8. Partial ^{1}H NMR spectra of probe RhPhCO6 with 80 equiv Na_2S as a function of time in MeOD-d_4/$CDCl_3$ (2:1, v/v).

9. Fluorescence spectra of Np-RhPhCO with various concentrations of Na_2S_2

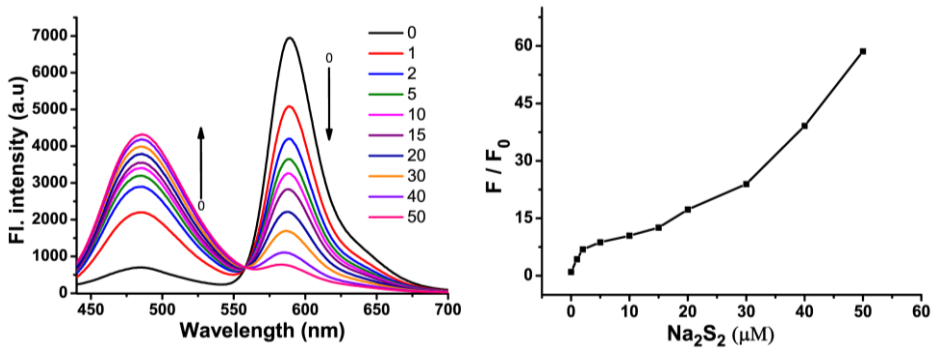

Fig. S9. Fluorescence spectra of **Np-RhPhCO** (5 μM) in the presence of various concentrations of Na_2S_2 (0, 1, 2, 5, 10, 15, 20, 30, 40, 50 μM, respectively) in MeCN/PBS = 4:6 (v/v, 25 mM, pH 7.4) buffer, at 37 °C. F and F_0 represent the fluorescence intensity ratio (I_{486}/I_{594}) in the presence and absence of Na_2S_2 respectively. λ_{ex} = 420 nm.

10. Fluorescence spectra of DSPE-Np-RhPhCO with various concentrations of Na_2S_2

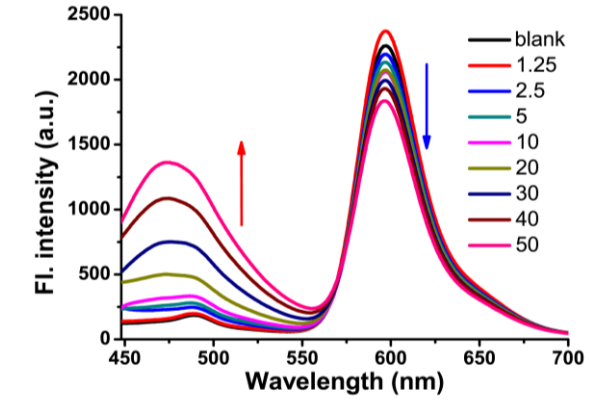

Fig. S10. Fluorescence spectra of **DSPE-Np-RhPhCO** (5 μM) in the presence of various concentrations of Na_2S_2 (0, 1.25, 2.5, 5, 10, 20, 30, 40, 50 μM, respectively) in PBS (pH 7.4) at 37 °C. λ_{ex} = 420 nm.

11. Absorption spectra and time-dependent fluorescence ratio changes of PPG-Np-RhPhCO reaction with Na_2S_2

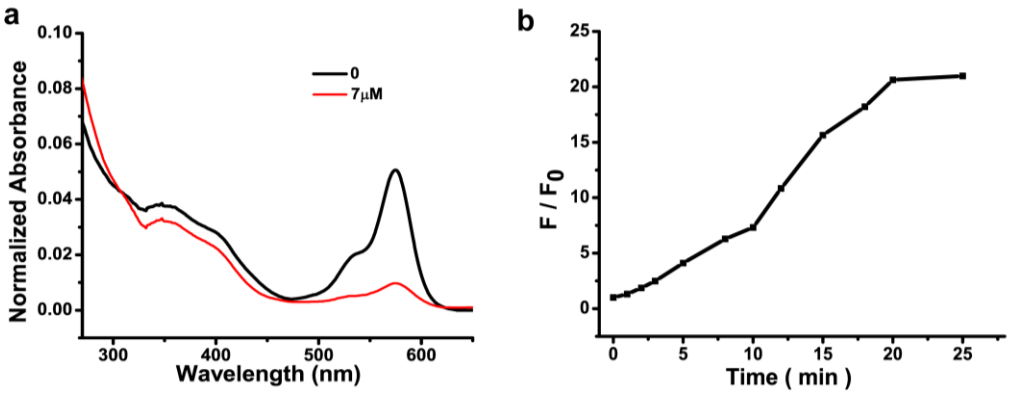

Fig. S11. (a) Absorption spectra of **PPG-Np-RhPhCO** in the presence of 7 μM Na_2S_2. (b). Time-dependent fluorescence ratio changes of **PPG-Np-RhPhCO** (4.8 μM) in the presence of Na_2S_2 (7 μM) in PBS (pH 7.4) at 37 °C. F and F_0 represent the fluorescence intensity ratio (I_{486}/I_{594}) in the presence and absence of Na_2S_2, respectively.

12. pH-dependent fluorescence ratio changes of PPG-Np-RhPhCO reaction with Na_2S_2 and TEM image

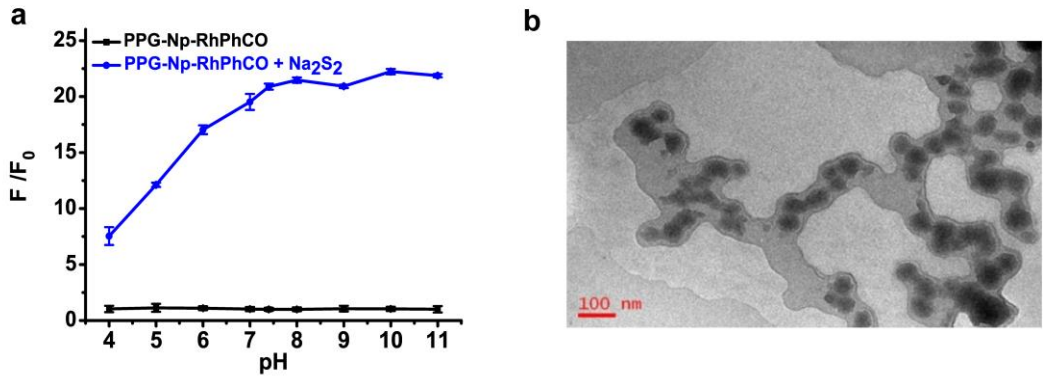

Fig. S12. (a) pH-dependent fluorescence ratio changes of **PPG-Np-RhPhCO** (4.8 μM) toward 7 μM Na_2S_2 in PBS buffer (25 mM, pH = 4.0-11.0), λ_{ex} = 420 nm. F and F_0 denoted the initial and final fluorescence intensity ratio (I_{486}/I_{594}), respectively; (b) Representative TEM image of **PPG-Np-RhPhCO**, the scale bar is 100 nm.

13. The stability of PPG-Np-RhPhCO

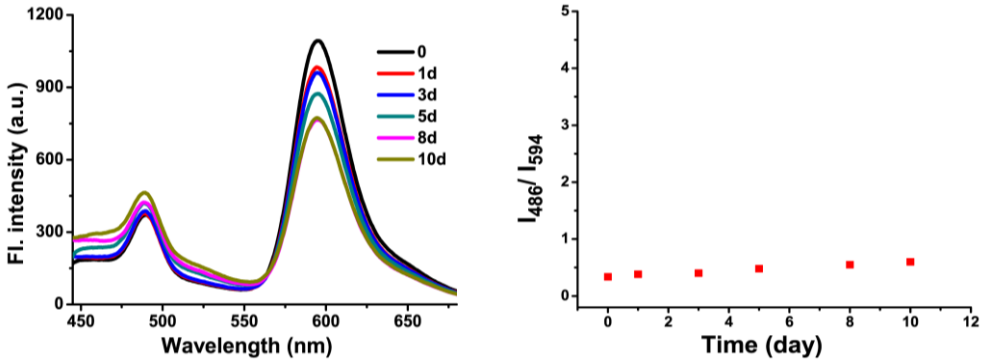

Fig. S13. Time-dependent fluorescence change of **PPG-Np-RhPhCO** (4.8 μM) in PBS buffer at room temperature. Note: minimal change was observed in the fluorescence ratio of the two emission bands at 486 and 594 nm (I_{486}/I_{594}), indicative of excellent stability of **PPG-Np-RhPhCO**. This result suggests the superiority of the probe **PPG-Np-RhPhCO** in bioimaging. λ_{ex} = 420 nm.

14. The cell viability of PPG-Np-RhPhCO in L02 cells

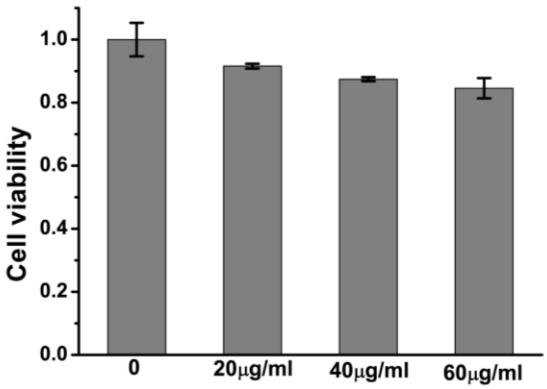

Fig. S14. MTT assay for estimating cell viability (%) of HL-7702 cells treated with various concentrations of nano-probe **PPG-Np-RhPhCO** (0-60 μg/mL). Error bars represent the standard deviations of three trials.

15. The photostability of PPG-Np-RhPhCO and Np-RhPhCO in live cells

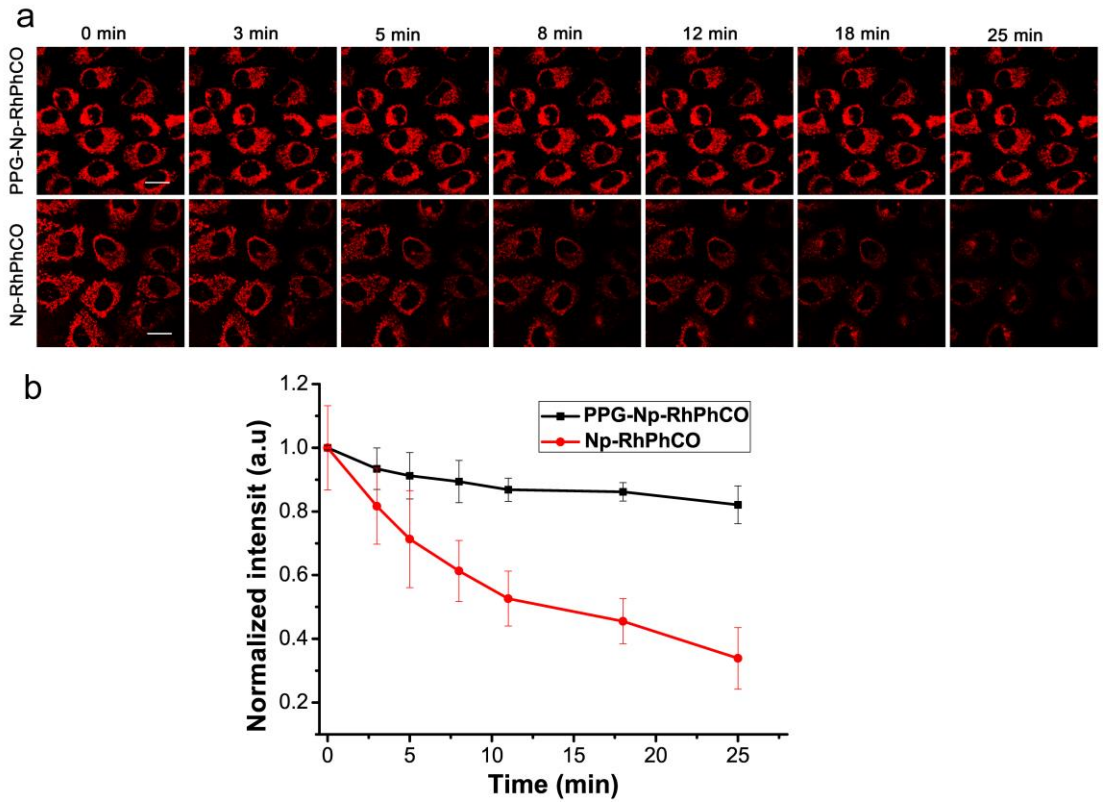

Fig. S15 (a) Confocal fluorescence images of live HL-7702 cells cultured with **PPG-Np-RhPhCO** (4.8 μM) and **Np-RhPhCO** (5.0 μM) with continuous irradiation using confocal microscope with the same parameters. (b) Quantification of the relative mean fluorescence levels of cells from the images of **PPG-Np-RhPhCO** and **Np-RhPhCO**. Scale bar: 20 μm. λ_{ex} = 405 nm, λ_{em} = 570-620 nm.

16. One-photon/Two-photon confocal microscopy images of H_2S_n in live cells with PPG-Np-RhPhCO

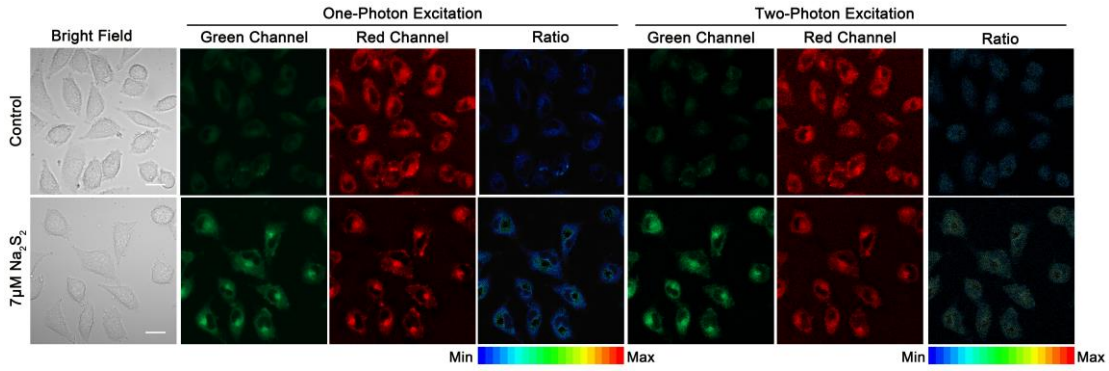

Fig. S16. One-photon/Two-photon confocal microscopy images of H_2S_n in live HL-7702 cell using nano-probe **PPG-Np-RhPhCO** (4.8 μM, 2 h). The first row: cells incubated with **PPG-Np-RhPhC**O for 2 h; the second row: cells incubated with **PPG-Np-RhPhCO** for 2 h, then 7 μM Na_2S_2 loaded for another 20 min; One-photon images were collected by the blue channel (425-475 nm) and the red channel (570-620 nm), respectively, upon excitation at 405 nm. Two-photon images were collected by the green channel (425-475 nm) and the red channel (570-620 nm), respectively, upon excitation at 820 nm. Ratio images generated from green channel to red channel.

17. Two-photon confocal microscopy images of H_2S_n in zebrafishes and tissues with PPG-Np-RhPhCO

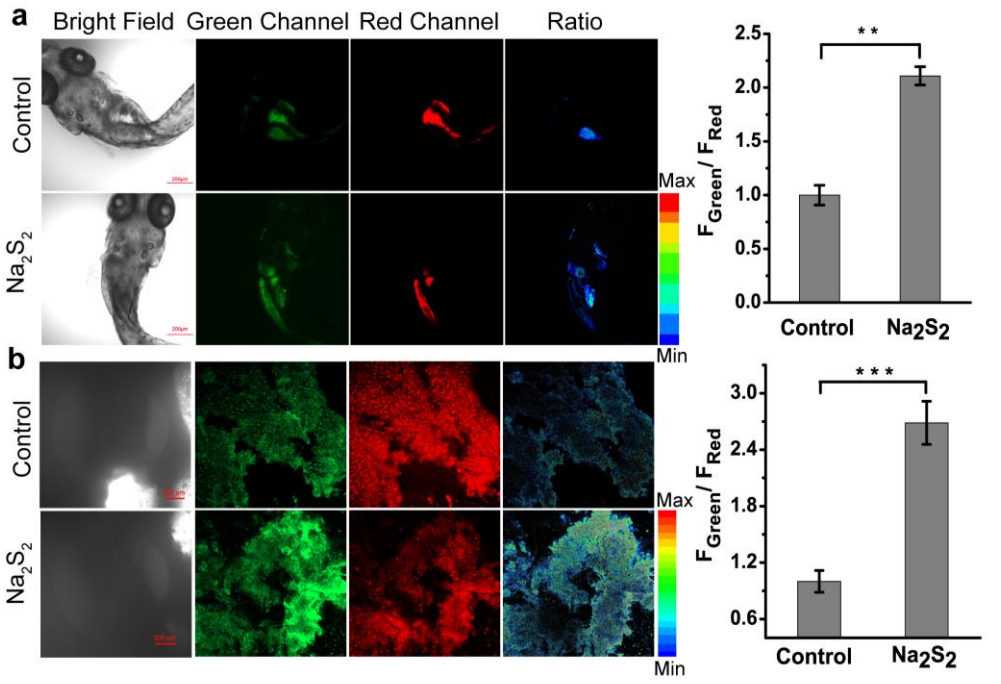

Fig. S17. Two-photon fluorescence images of H_2S_n in zebrafishes and fresh tissues using nano-probe **PPG-Np-RhPhCO** (14.4 μM) for 4 h in with a magnification of 10×: (a) The control group zebrafishes treated only **PPG-Np-RhPhCO** for 2 h; (b) The other group zebrafishes incubated with **PPG-Np-RhPhCO** for 2 h and then treated with 30 μM Na_2S_2 for 30 min; (c) The control group tissues treated only **PPG-Np-RhPhCO** for 4 h; (d) The other group liver tissues incubated with **PPG-Np-RhPhCO** for 4 h and then treated with 30 μM Na_2S_2 for 1 h; (e, f) Average ratio values of fluorescence intensity (F_{Green} /F_{Red}) in panel A. Excitation: 780 nm. Emission band at 425-475 nm in the green channel and 570-620 nm in the red channel. Zebrafishes and fresh tissues shown are representative images from replicate experiments (n = 5 independent experiments). Scale bar: 200 μm.

18. Oil Red O staining and intracellular TG measurement of L02 cells in NAFLD model

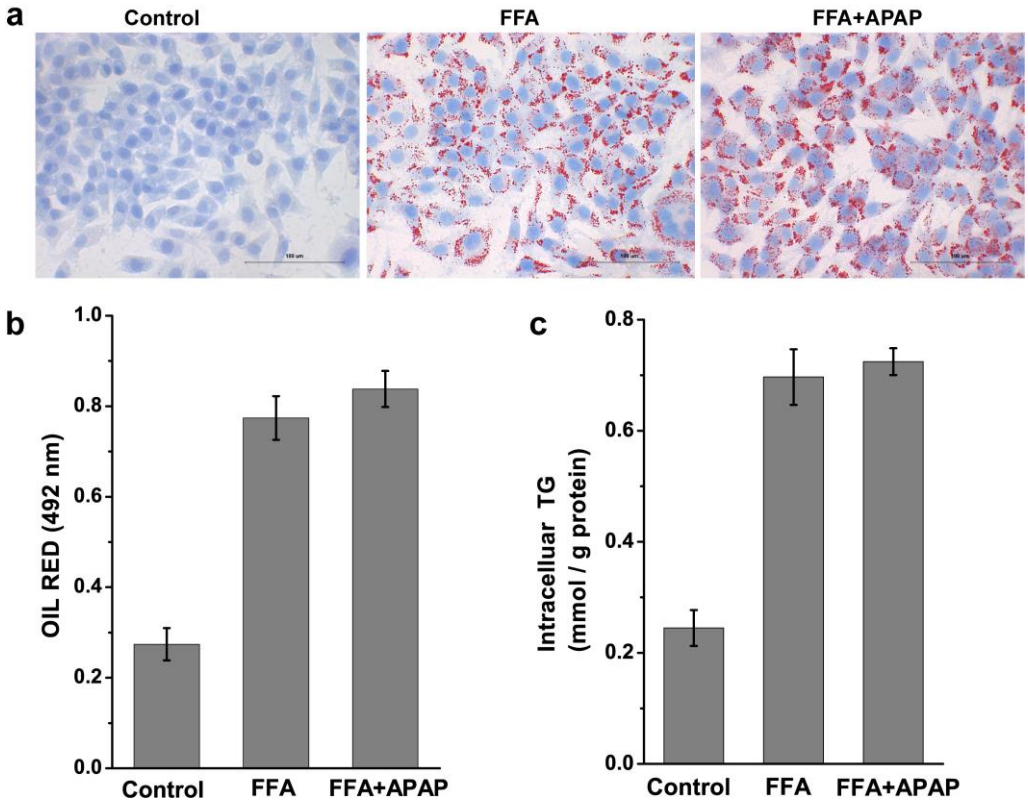

Fig. S18. (a). Representative images of Oil Red O staining of L02 cells. Scale bar: 100 μm. (b). Staining was quantified by spectrophotometric analysis at 492 nm. (c). The intracellular TG measurement of L02 cells.

19. Endogenous H_2S detection and imaging of L02 cells in NAFLD model with probe TPC-N_3

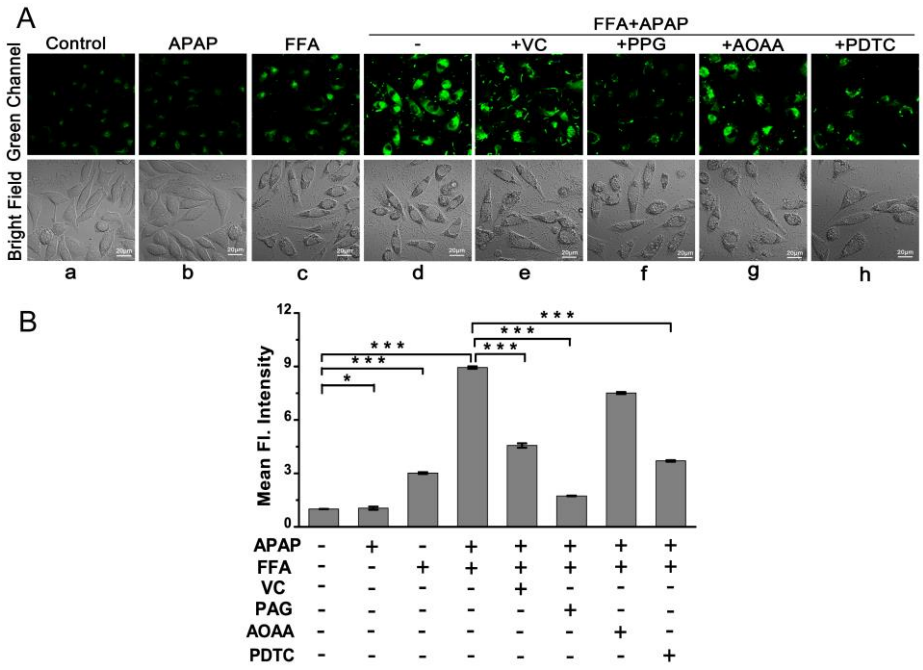

Fig. S19. (A) Fluorescence images of probe TPC-N_3 in HL-7702 cells under different conditions by confocal fluorescence images. (a) Cells were incubated with probe TPC-N_3 (5 μM) for 30 min, then imaged. (b, c) Cells were pre-stimulated with APAP or FFA, respectively, and then treated as (a). (d) Cells were pretreated with FFA, and then treated as (b). (e) Cells were pretreated with FFA, then pre-stimulated with VC and then treated as (b). (f, g, h) Cells were pretreated with FFA, then pre-stimulated with PPG or AOAA or PDTC, and then treated as (b). The fluorescence images were captured from the green channel of 500-550 nm with an excitation at 405 nm. (B) Average fluorescence intensity of in panel (A). Data are mean ± S.E.M., n = 3 independent experiments, 70 cells. Statistical significance were calculated with unpaired two-tailed Student's *t*-tests. * $p < 0.05$, *** $p < 0.001$. Scale bar: 20 μm.

20. Endogenous $ONOO^-$ (ROS) detection and imaging of L02 cells in NAFLD model with probe MITO-CC

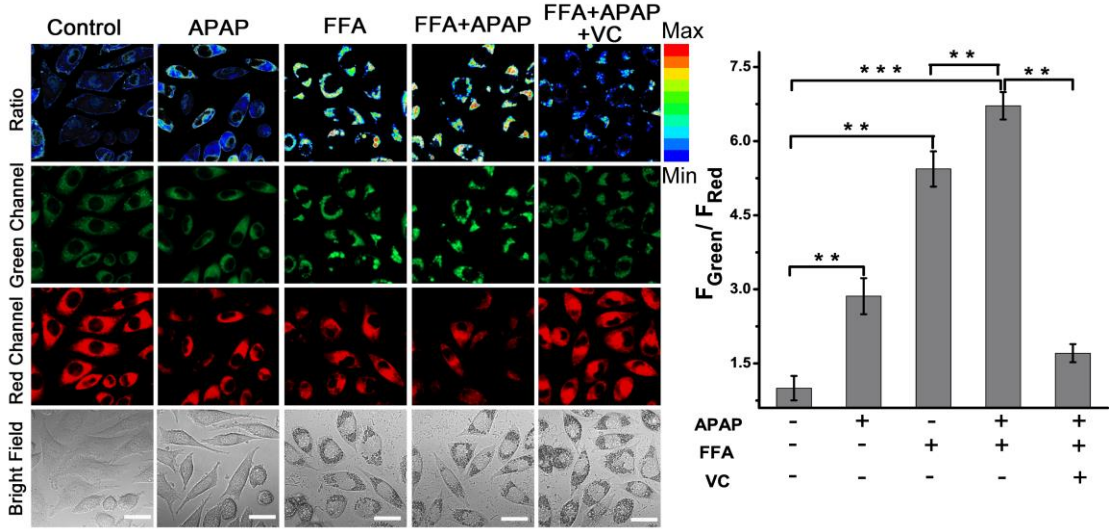

Fig. S20. Fluorescence images of probe MITO-CC (5 μM) in HL-7702 cells under different conditions by confocal fluorescence images. The first column: incubation with MITO-CC for 30 min, then imaged; the second and third column: incubation with MITO-CC for 30 min after treatment with APAP (3 mM) for 12 h or FFA (0.5 mM) for 12 h respectively; the fourth and fifth column: pretreatment with FFA (0.5 mM) for 12 h, and incubation with APAP (3 mM) for 12 h, then incubation with MITO-CC for 30 min; the fifth column: pretreatment with FFA (0.5 mM) for 12 h and then treatment with VC (1 mM) for 2 h, and incubation with APAP (3 mM) for 12 h before incubation with MITO-CC for 30 min. The fluorescence images were captured from the green channel of 425-475 nm and red channel of 660-730 nm with an excitation at 405 nm. Ratio: F_{Green}/F_{Red} ratiometric images. Average fluorescence intensity ratios (F_{Green}/F_{Red}). Data are mean ± S.E.M., n = 5 independent experiments, 80 cells. Statistical significance were calculated with unpaired two-tailed Student's *t*-tests. ** $p < 0.01$, *** $p < 0.001$. Scale bar: 20 μm.

21. Endogenous H_2S_n detection and imaging of L02 cells stimulated at different drug concentrations with probe PPG-Np-RhPhCO

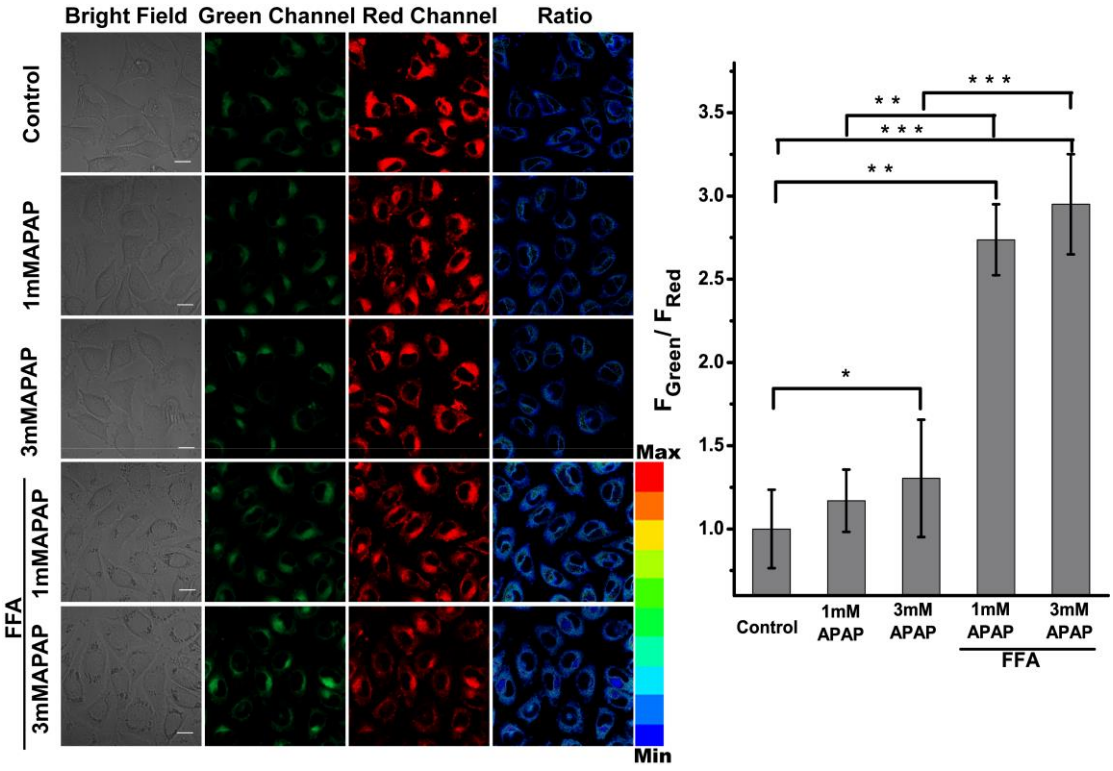

Fig. S21. Fluorescence images of 4.8 μM nano-probe **PPG-Np-RhPhCO** in HL-7702 cells under different conditions by confocal fluorescence images. The first line: Cells were incubated with **PPG-Np-RhPhCO** for 2 h, then imaged. The second and third line: Cells were pre-stimulated with 1 mM or 3 mM APAP for 12 h, and then treated as the first line. The fourth and fifth line: Cells pretreated with 0.5 mM FFA for 12 h, then pre-stimulated with 1 mM or 3 mM APAP for 12 h and then treated as the first line. The fluorescence images were captured from the green channel of 425-475 nm and red channel of 570-620 nm with an excitation at 405 nm. Ratio: F_{Green}/F_{Red} ratiometric images. Average fluorescence intensity ratios (F_{Green}/F_{Red}). Data are mean ± S.E.M., n = 5 independent experiments, 70 cells. Statistical significance were calculated with unpaired two-tailed Student's *t*-tests. * $p < 0.05$, ** $p < 0.01$, *** $p < 0.001$. Scale bar: 20 μm.

22. Endogenous H_2S_n detection and tissue imaging in animal model of NAFLD with probe PPG-Np-RhPhCO

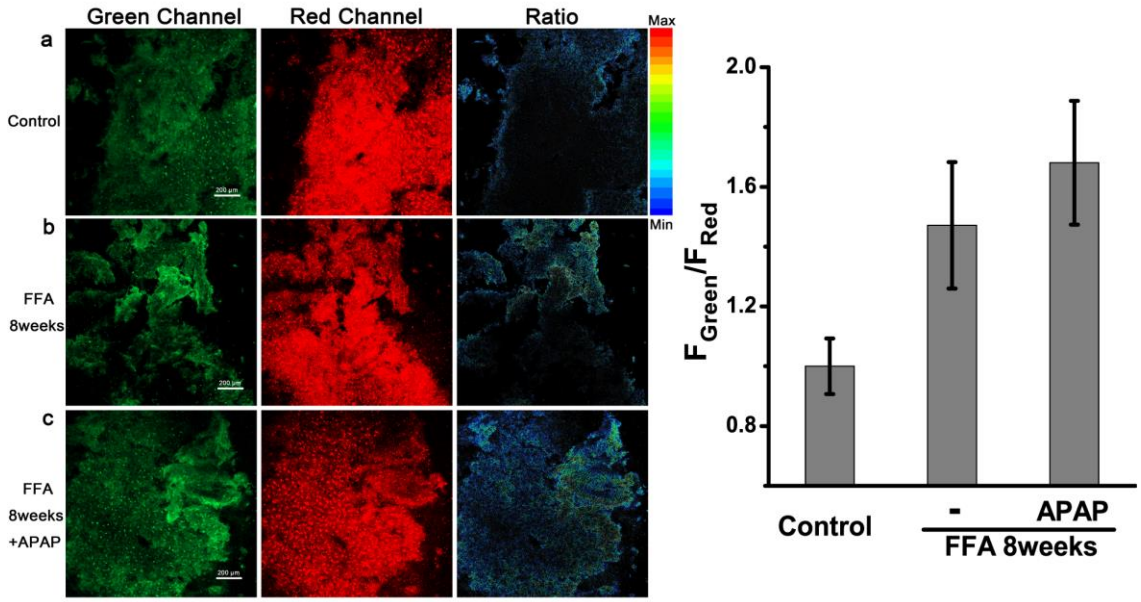

Fig. S22. Two-photon fluorescence images of fresh liver tissues of HFD-fed mice treated with nanoprobe PPG-Np-RhPhCO (14.4 μM) for 4 h: (a) Normal mice liver tissue treated with PPG-Np-RhPhCO; (b) mice (HFD-fed after 8 weeks) liver tissue treated with PPG-Np-RhPhCO; (c) mice (HFD-fed after 8 weeks and APAP for 6 h) liver tissue treated with PPG-Np-RhPhCO. (d) Average fluorescence intensity ratios (F_{Green}/F_{Red}) of lives tissue under the conditions in (a-c). Data represent mean standard error (n = 3 independent experiments). Excitation: 780 nm. Emission band at 425-475 nm in the green channel and 570-620 nm in the red channel. Scale bar: 200 μm.

23. Supplemental References

1. M. J. Frisch, et al. Gaussian 09, Revision A.1, Gaussian, Inc. Wallingford, CT, 2009.
2. R. Kawagoe, I. Takashima, S. Uchinomiya, A. Ojida, *Chem. Sci.* 2017, **8**, 1134-1140.
3. M. Li, C. Xu, J. Shi, J. Ding, X. Wan, D. Chen, J. Gao, C. Li, J. Zhang, Y. Lin, Z. Tu, X. Kong, Y. Li and C. Yu, *Gut*, 2018, **67**, 2169-2180.
4. E. D. Parker, P. E. Deal, R. U. Kulkarni, S. H. Al-Abdullatif, E. W. Miller, *J. Am. Chem. Soc.* 2016, **138**, 9085-9088.
5. L. Zhou, X. Zhang, Q. Wang, Y. Lv, G. Mao, A. Luo, Y. Wu, Y. Wu, J. Zhang, W. Tan, *J. Am. Chem. Soc.* 2014, **136**, 9838-9841.

24. NMR and MS spectra of synthesis compounds

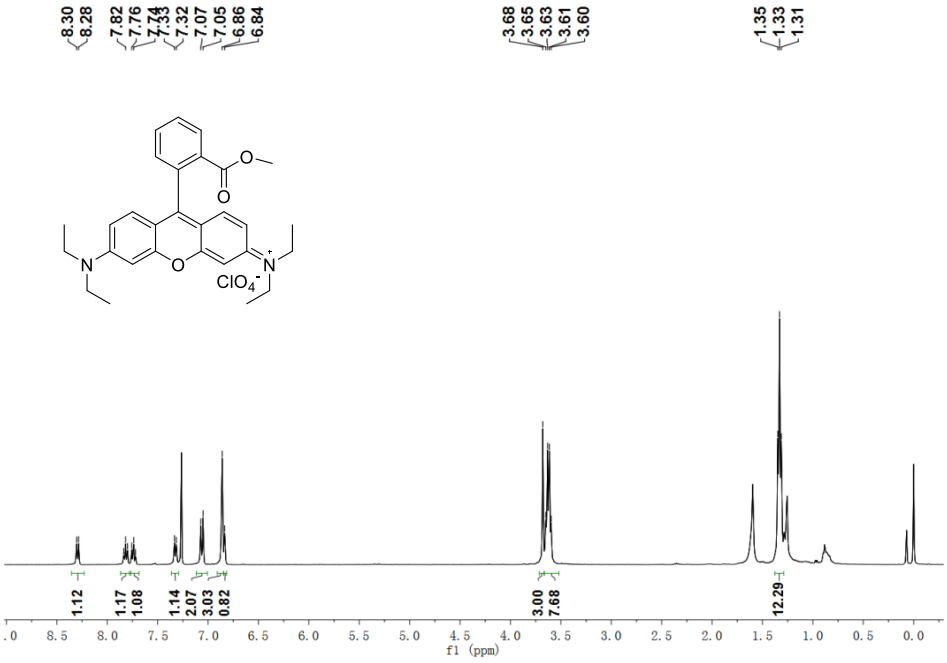

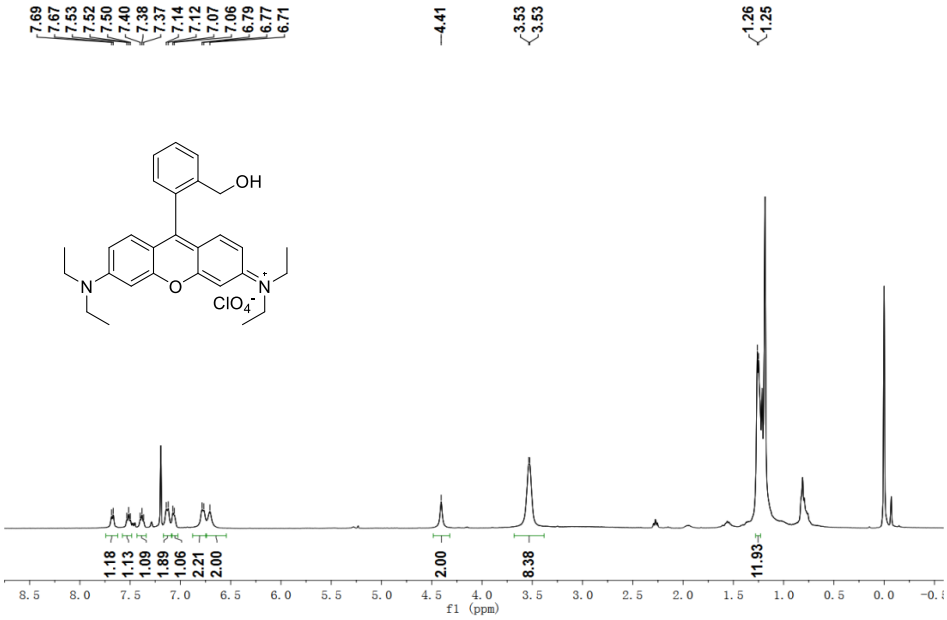

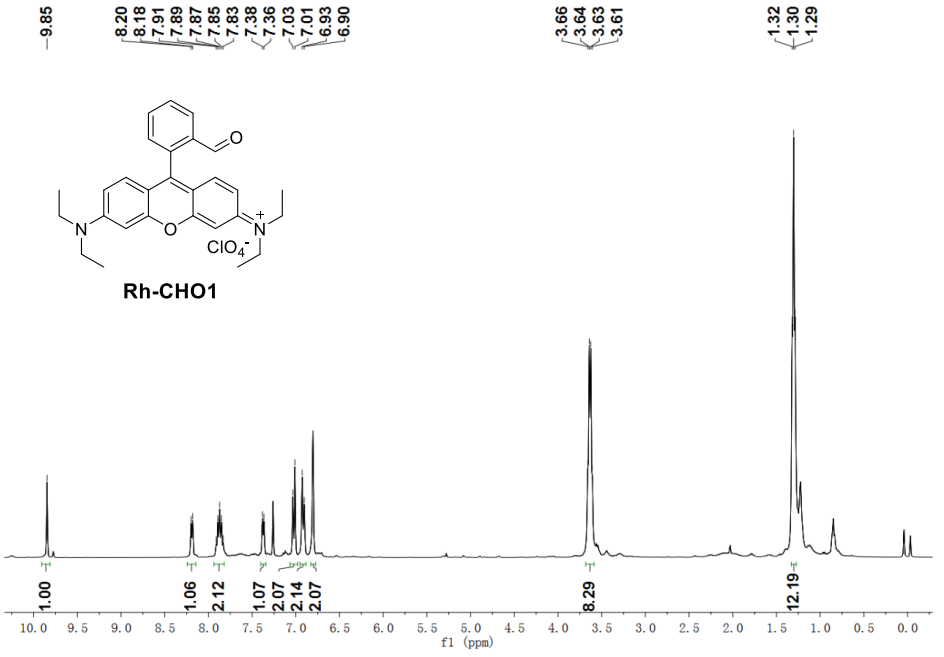

Rh-CHO1

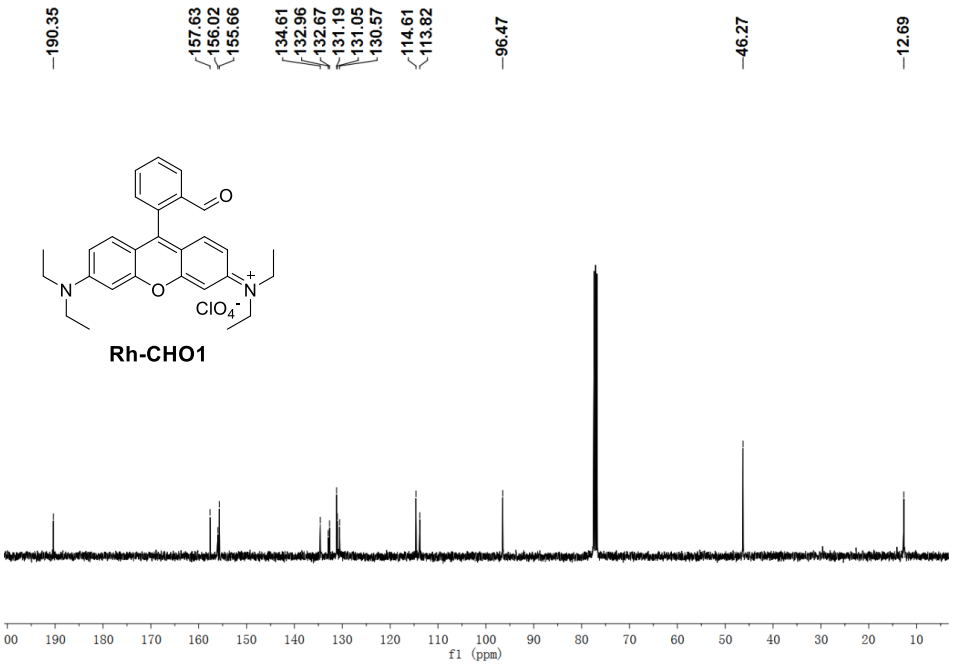

Rh-CHO1

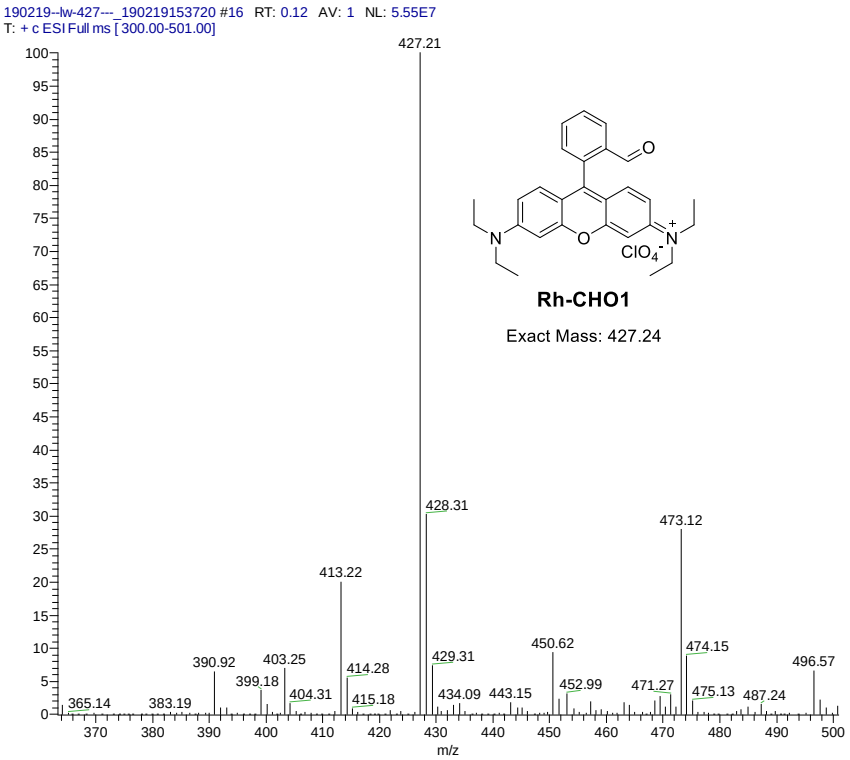
190219--lw-427---_190219153720 #16 RT: 0.12 AV: 1 NL: 5.55E7
T: + c ESI Full ms [300.00-501.00]
427.21
428.31
473.12
413.22
450.62
474.15
496.57
390.92
403.25
414.28
429.31
399.18
404.31
415.18
434.09
443.15
452.99
471.27
475.13
487.24
365.14
383.19
m/z
Rh-CHO1
Exact Mass: 427.24

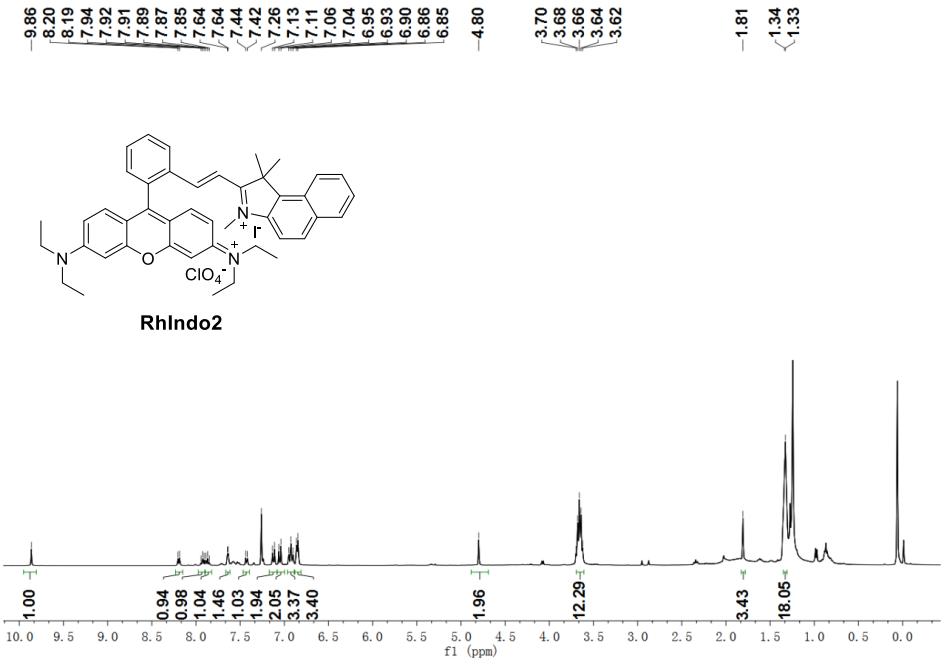
9.86
8.20
8.19
7.94
7.92
7.91
7.89
7.87
7.85
7.64
7.64
7.44
7.42
7.26
7.13
7.11
7.06
7.04
6.95
6.93
6.90
6.86
6.85
4.80
3.70
3.68
3.66
3.64
3.62
1.81
1.34
1.33
RhIndo2
1.00
0.94
0.98
1.04
1.46
1.03
1.94
2.05
3.37
3.40
1.96
12.29
3.43
18.05
f1 (ppm)

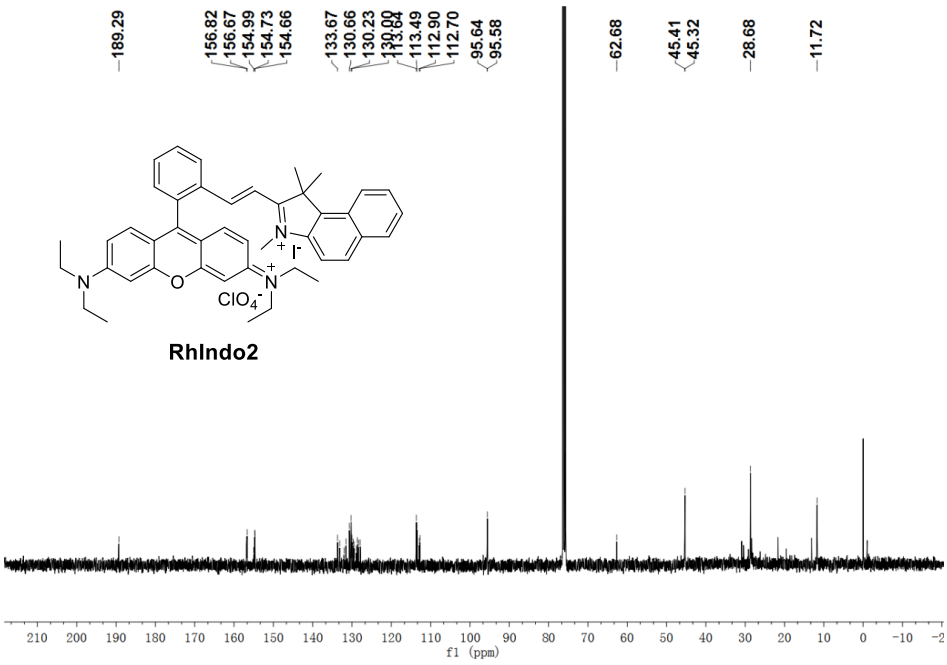

RhIndo2

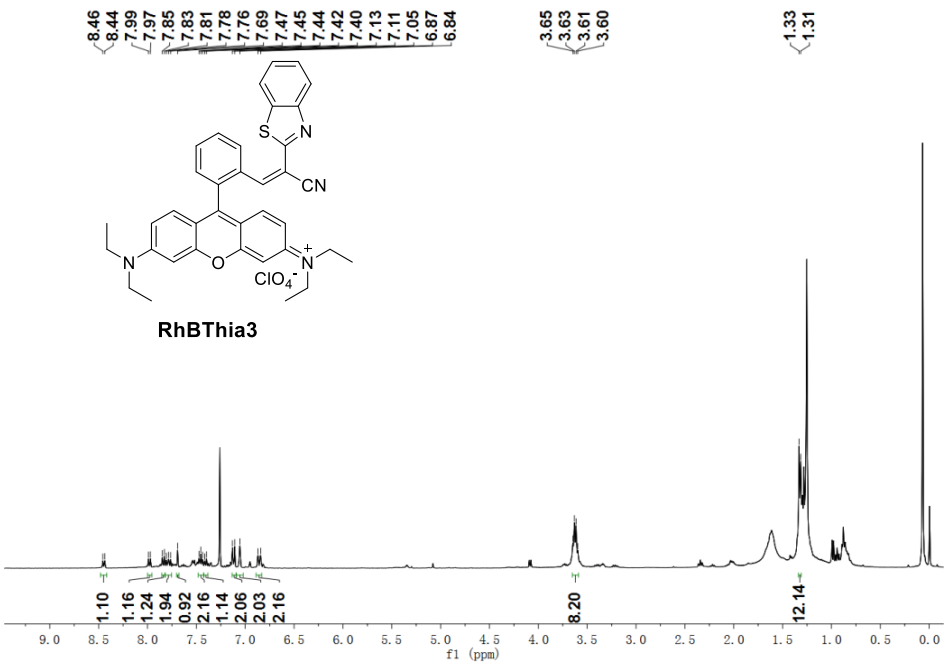

RhBThia3

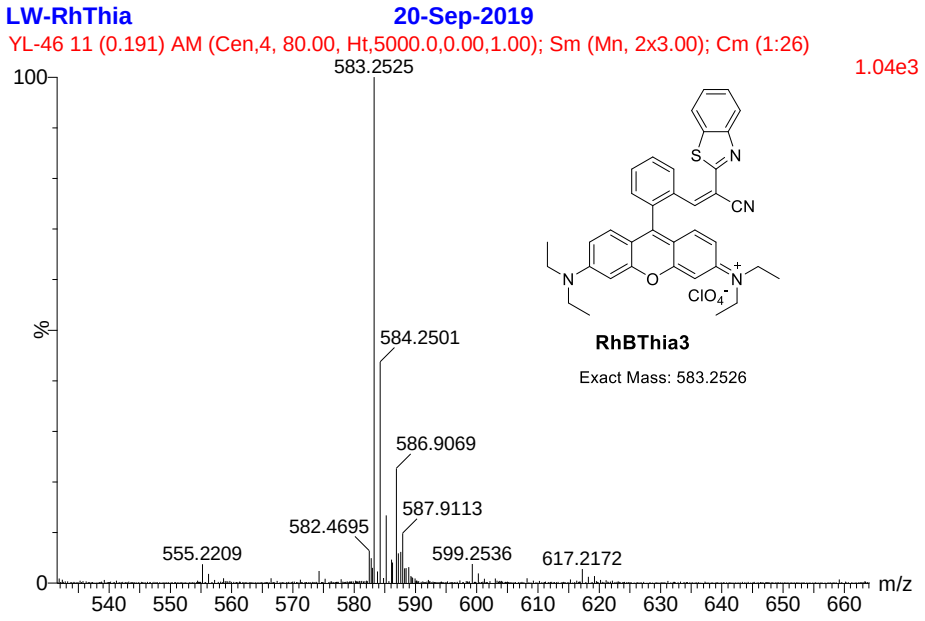
LW-RhThia
20-Sep-2019
YL-46 11 (0.191) AM (Cen,4, 80.00, Ht,5000.0,0.00,1.00); Sm (Mn, 2x3.00); Cm (1:26)
1.04e3
583.2525
584.2501
586.9069
587.9113
582.4695
555.2209
599.2536
617.2172
RhBThia3
Exact Mass: 583.2526
m/z

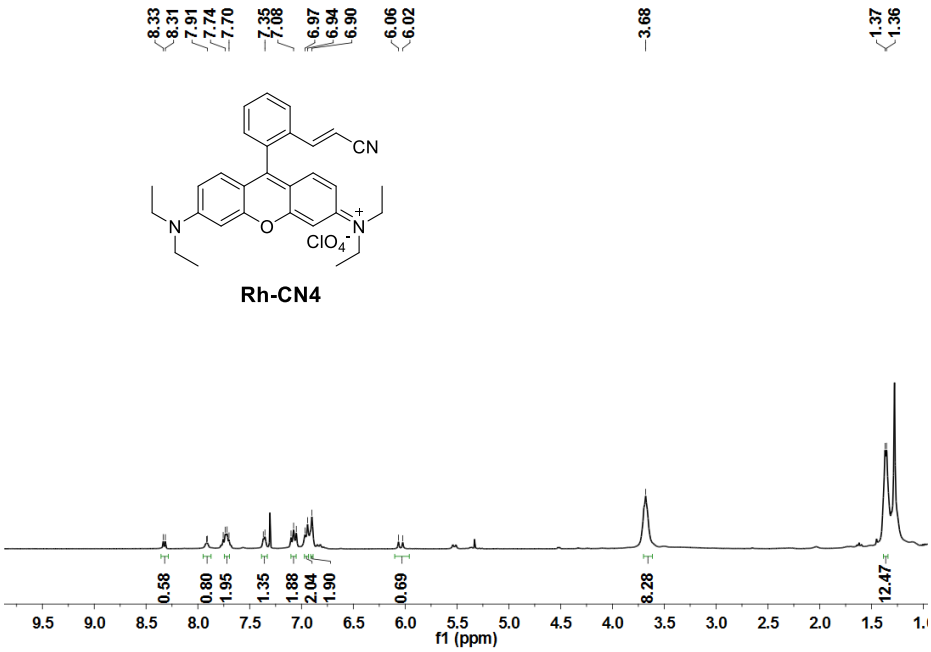
8.33
8.31
7.91
7.74
7.70
7.35
7.08
6.97
6.94
6.90
6.06
6.02
3.68
1.37
1.36
Rh-CN4
0.58
0.80
1.95
1.35
1.88
2.04
1.90
0.69
8.28
12.47
f1 (ppm)

LW-RhCN **20-Sep-2019**

YL-45 8 (0.137) AM (Cen,4, 80.00, Ht,5000.0,0.00,1.00); Sm (Mn, 2x3.00); Cm (1:31)

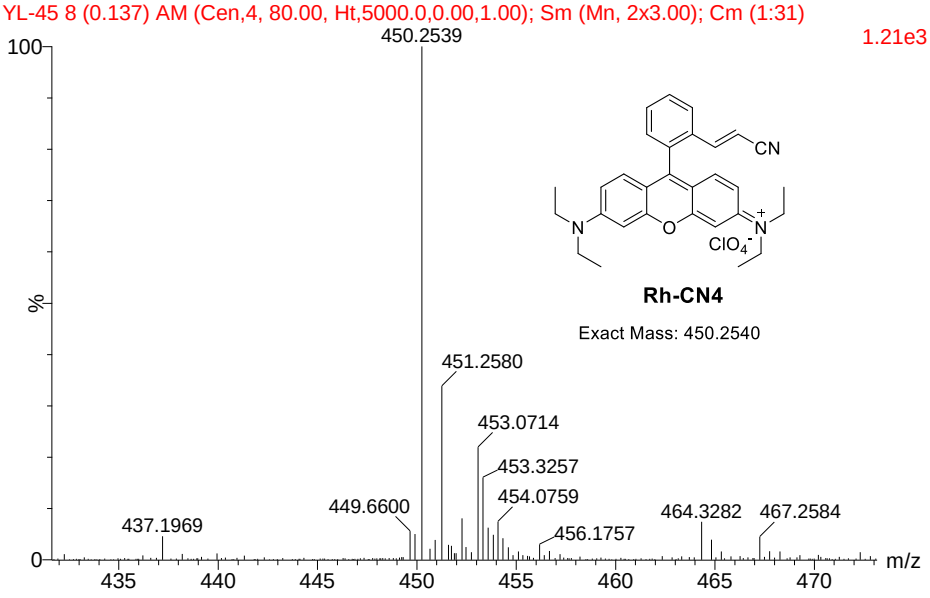

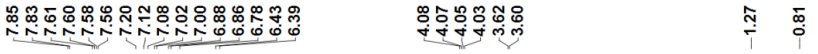

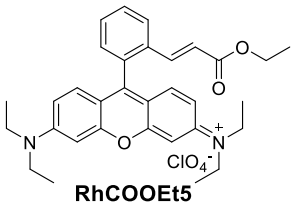

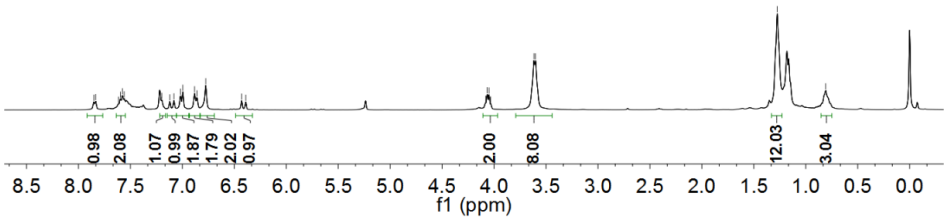

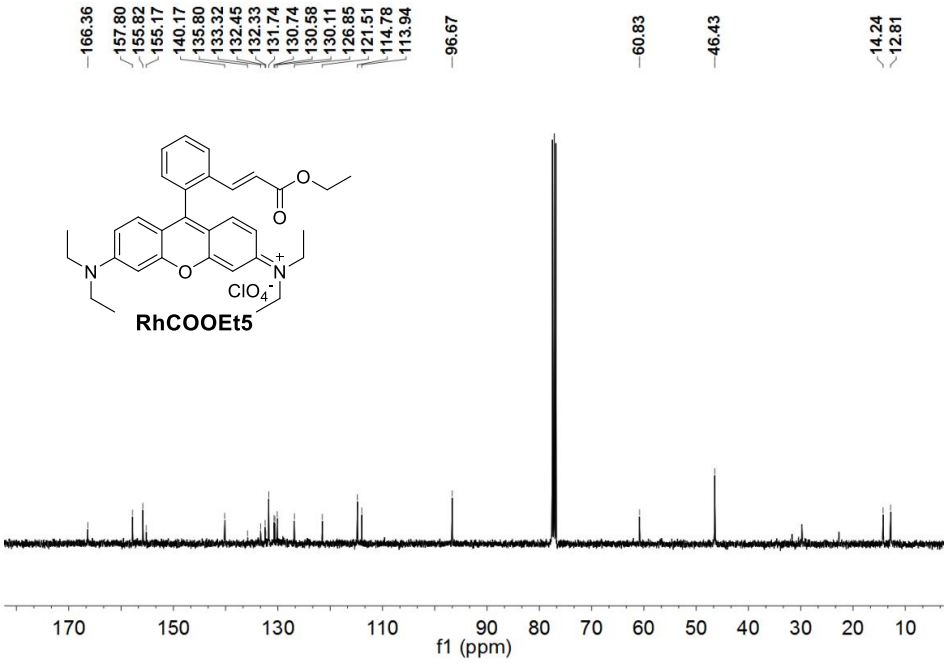
166.36
157.80
155.82
155.17
140.17
135.80
133.32
132.45
132.33
131.74
130.74
130.58
130.11
126.85
121.51
114.78
113.94
96.67
60.83
46.43
14.24
12.81
RhCOOEt5
170
150
130
110
90
80
70
60
50
40
30
20
10
f1 (ppm)

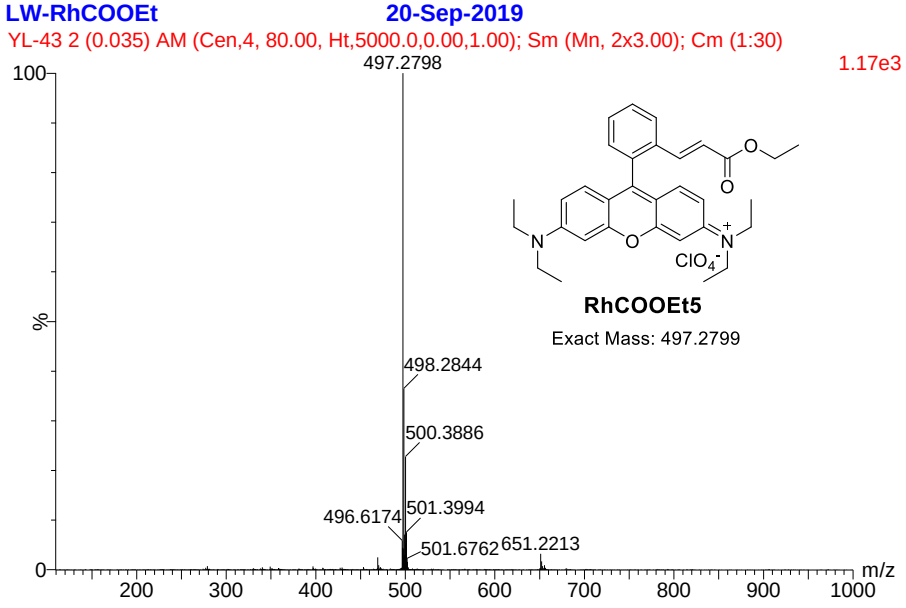
LW-RhCOOEt
20-Sep-2019
YL-43 2 (0.035) AM (Cen,4, 80.00, Ht,5000.0,0.00,1.00); Sm (Mn, 2x3.00); Cm (1:30)
1.17e3
497.2798
100
%
0
498.2844
500.3886
496.6174
501.3994
501.6762
651.2213
RhCOOEt5
Exact Mass: 497.2799
200
300
400
500
600
700
800
900
1000
m/z

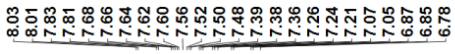

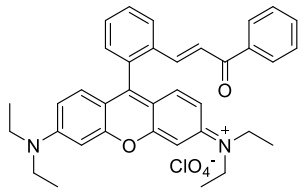

RhPhCO6

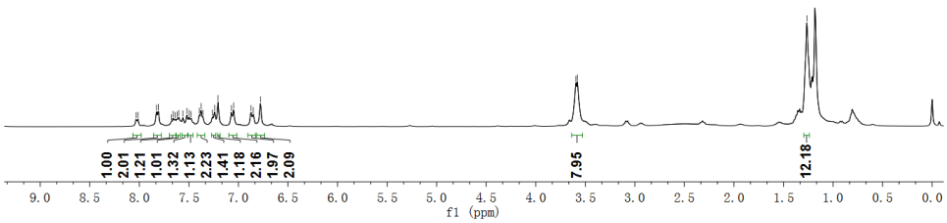

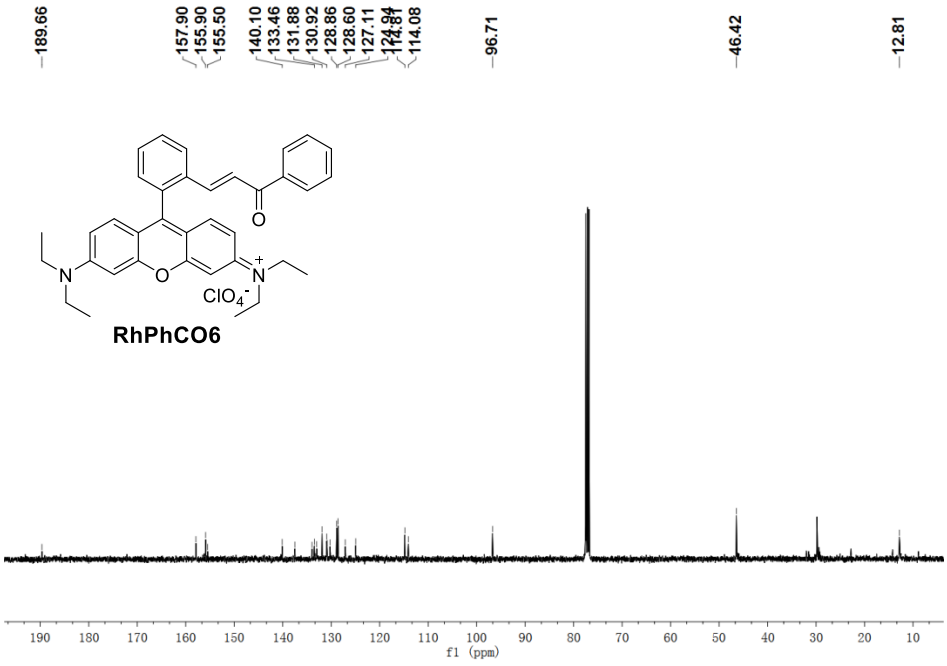

RhPhCO6

LW-RHPHCO **20-Sep-2019**

YL-42 11 (0.190) AM (Cen,4, 80.00, Ht,5000.0,0.00,1.00); Sm (Mn, 2x3.00); Cm (1:11)

739

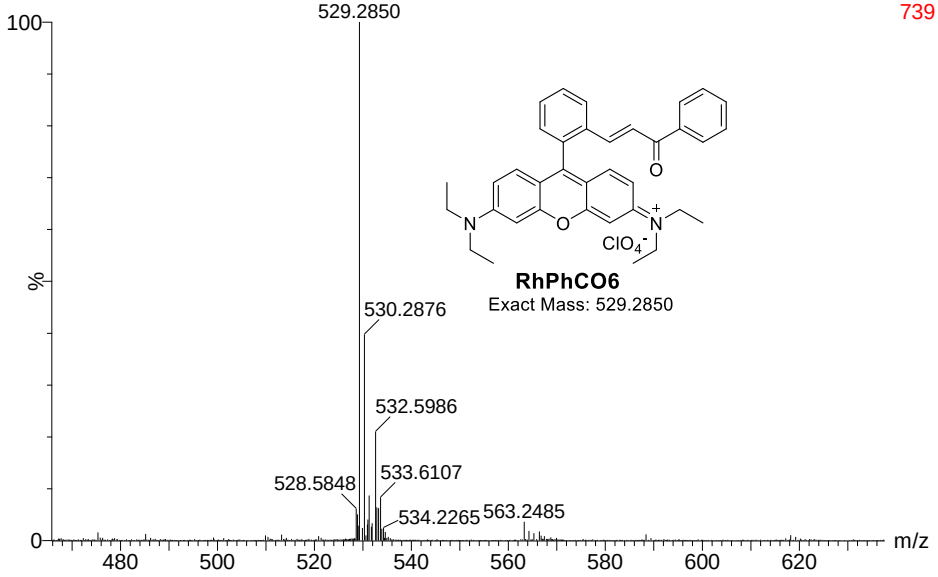

RhPhCO6

Exact Mass: 529.2850

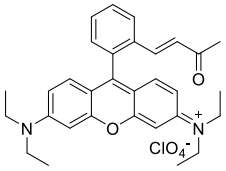

RhAceton7

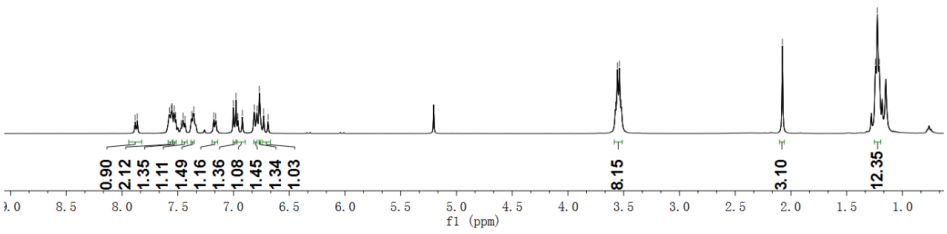

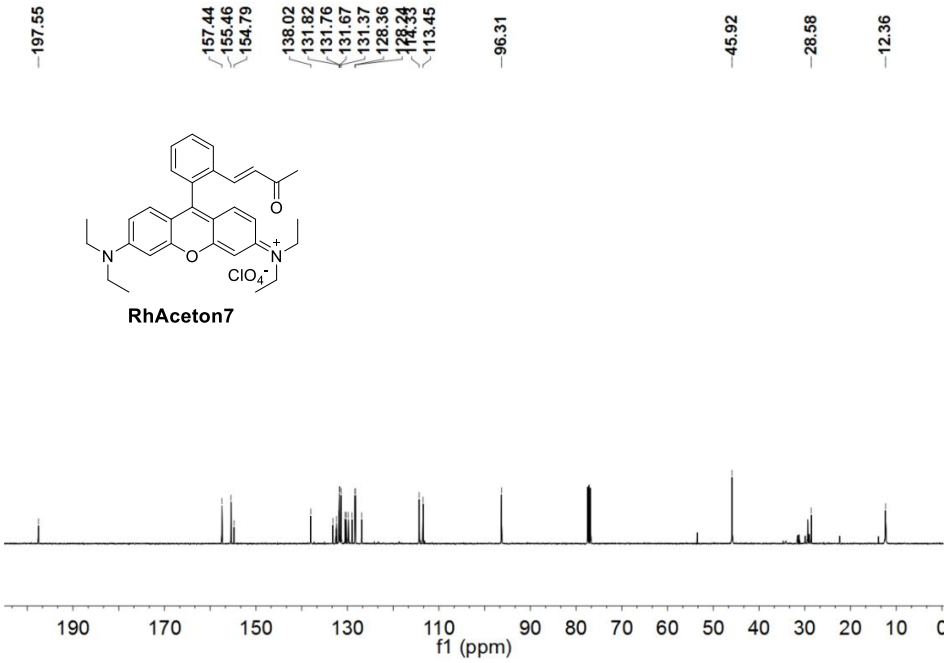
197.55
157.44
155.46
154.79
138.02
131.82
131.76
131.67
131.37
128.36
96.31
45.92
28.58
12.36
RhAceton7
190
170
150
130
110
90
80
70
60
50
40
30
20
10
f1 (ppm)

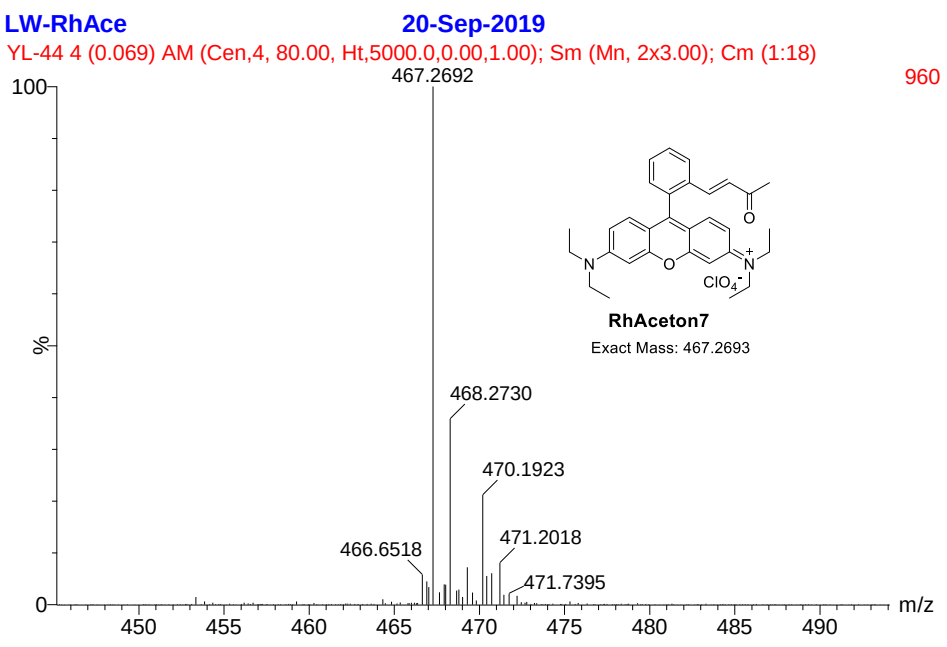
LW-RhAce
20-Sep-2019
YL-44 4 (0.069) AM (Cen,4, 80.00, Ht,5000.0,0.00,1.00); Sm (Mn, 2x3.00); Cm (1:18)
960
467.2692
100
%
0
468.2730
470.1923
471.2018
466.6518
471.7395
RhAceton7
Exact Mass: 467.2693
450
455
460
465
470
475
480
485
490
m/z

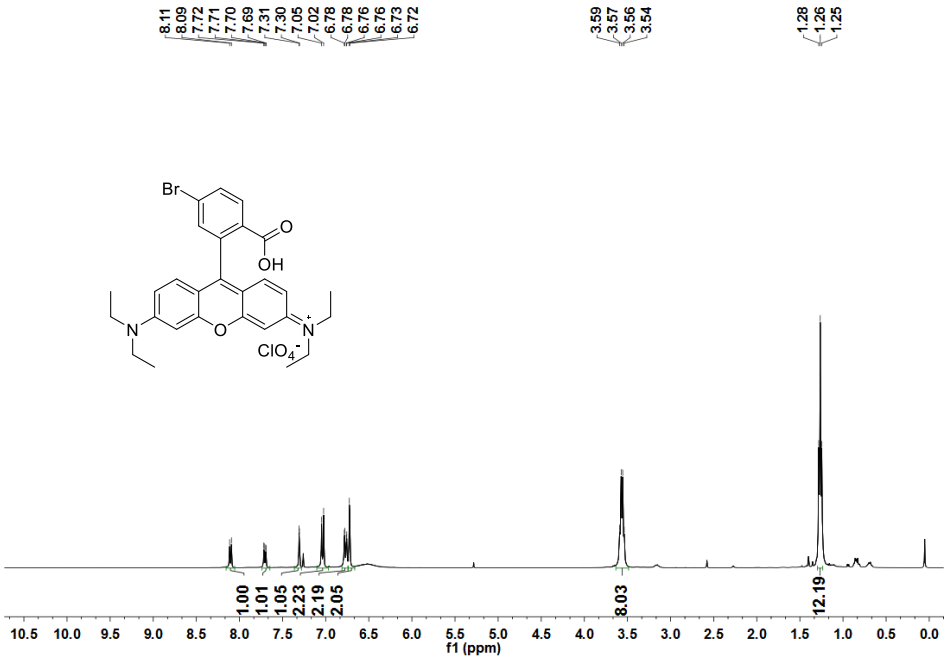
8.11
8.09
7.72
7.71
7.70
7.69
7.31
7.30
7.05
7.02
6.78
6.78
6.76
6.76
6.73
6.72
3.59
3.57
3.56
3.54
1.28
1.26
1.25
Br
O
OH
N
O
N
ClO4-
1.00
1.01
1.05
2.23
2.19
2.05
8.03
12.19
f1 (ppm)

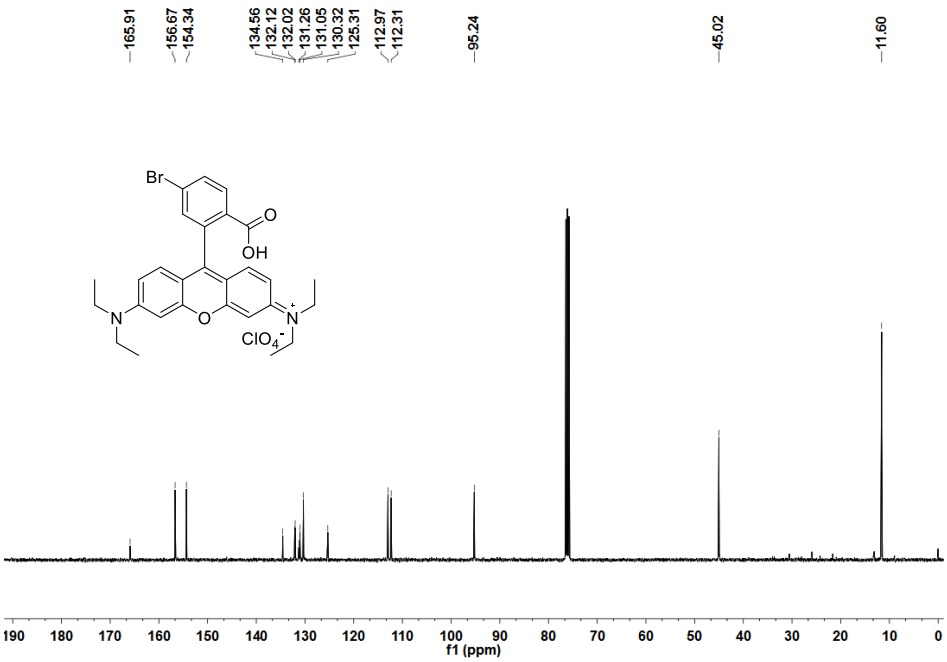
165.91
156.67
154.34
134.56
132.12
132.02
131.26
131.05
130.32
125.31
112.97
112.31
95.24
45.02
11.60
Br
O
OH
N
O
N
ClO4-
f1 (ppm)

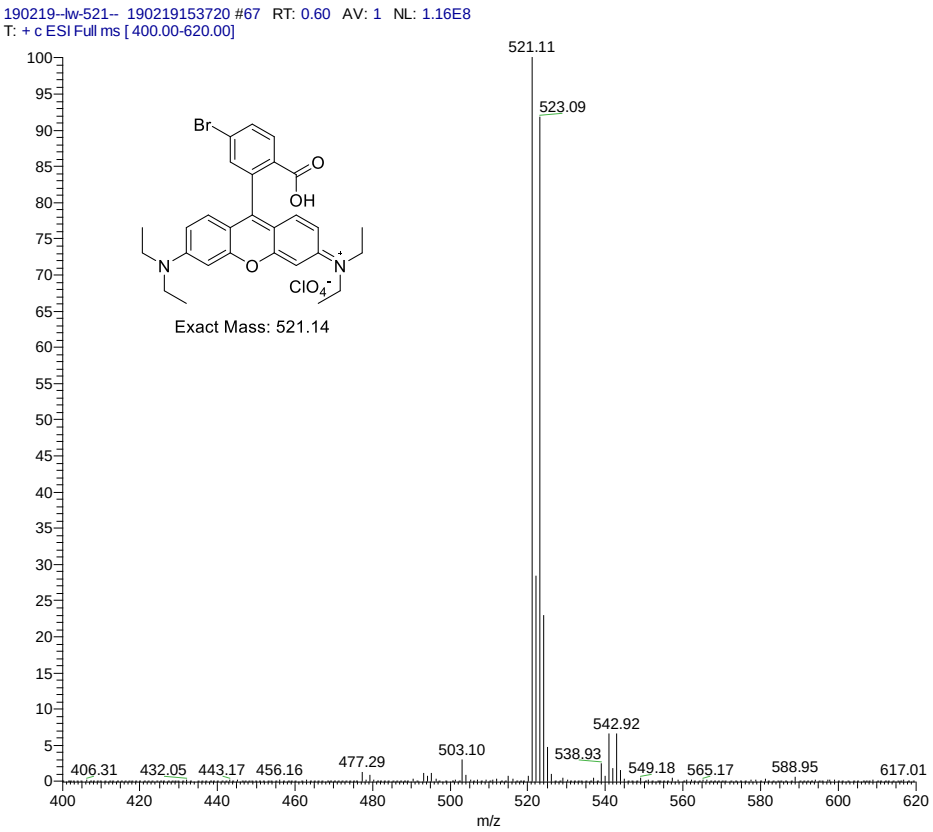
190219--lw-521-- 190219153720 #67 RT: 0.60 AV: 1 NL: 1.16E8
T: + c ESI Full ms [400.00-620.00]
521.11
523.09
542.92
503.10
538.93
477.29
406.31
432.05
443.17
456.16
549.18
565.17
588.95
617.01
m/z
Exact Mass: 521.14

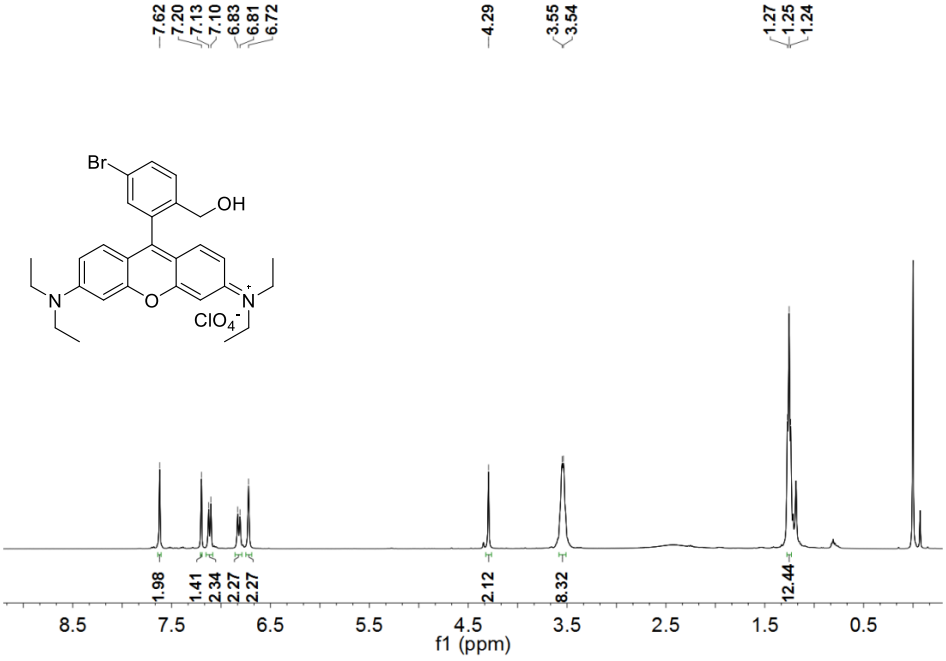
7.62
7.20
7.13
7.10
6.83
6.81
6.72
4.29
3.55
3.54
1.27
1.25
1.24
1.98
1.41
2.34
2.27
2.27
2.12
8.32
12.44
f1 (ppm)

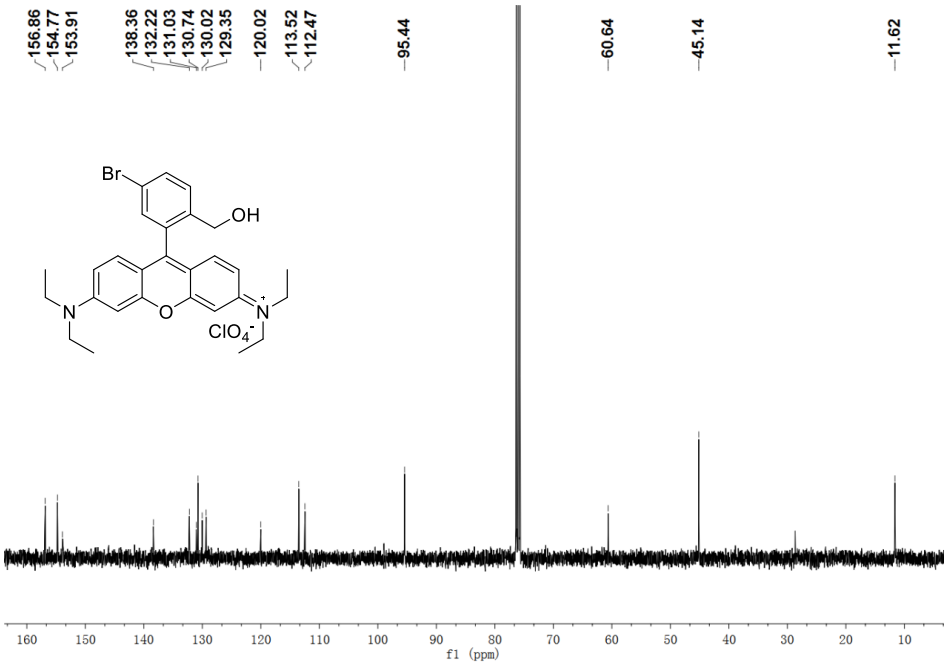
156.86
154.77
153.91
138.36
132.22
131.03
130.74
130.02
129.35
120.02
113.52
112.47
95.44
60.64
45.14
11.62
Br
OH
N
O
N
ClO4-
160
150
140
130
120
110
100
90
80
70
60
50
40
30
20
10
f1 (ppm)

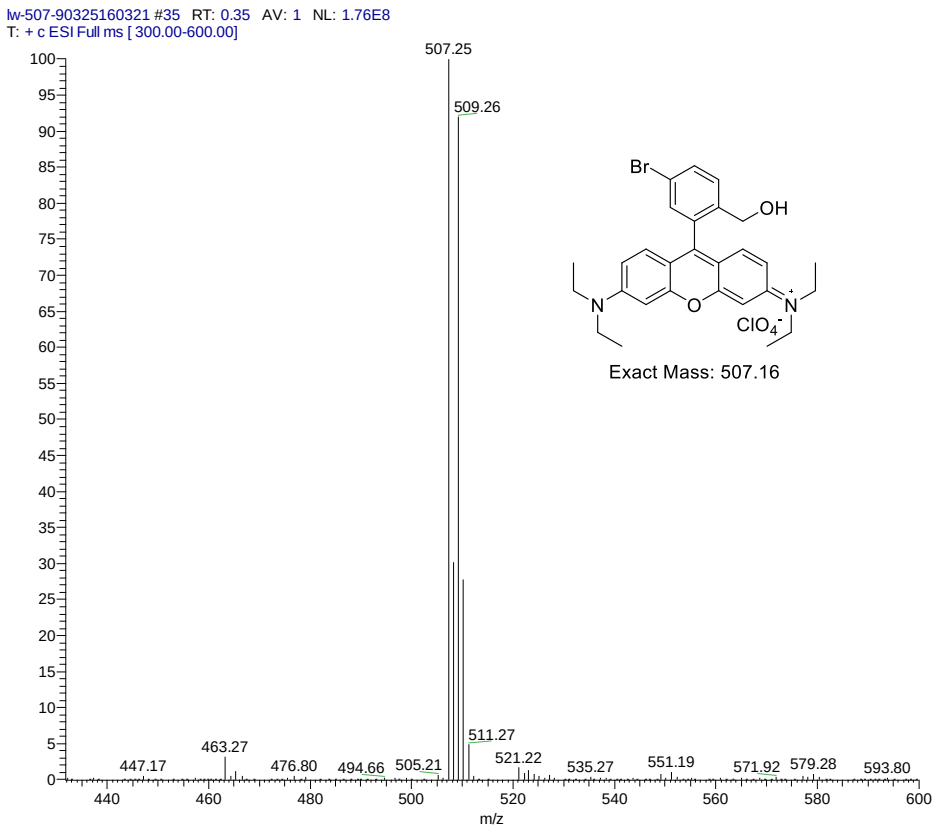
lw-507-90325160321 #35 RT: 0.35 AV: 1 NL: 1.76E8
T: + c ESI Full ms [300.00-600.00]
507.25
509.26
511.27
463.27
447.17
476.80
494.66
505.21
521.22
535.27
551.19
571.92
579.28
593.80
Br
OH
N
O
N
ClO4-
Exact Mass: 507.16
m/z

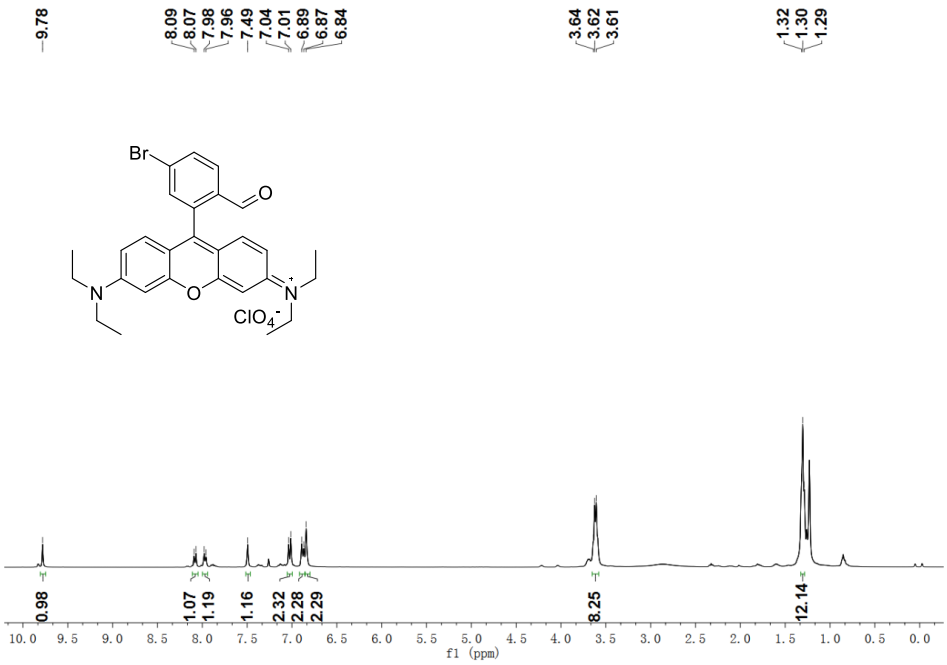
9.78
8.09
8.07
7.98
7.96
7.49
7.04
7.01
6.89
6.87
6.84
3.64
3.62
3.61
1.32
1.30
1.29
Br
O
N
O
N
ClO4-
0.98
1.07
1.19
1.16
2.32
2.28
2.29
8.25
12.14
f1 (ppm)

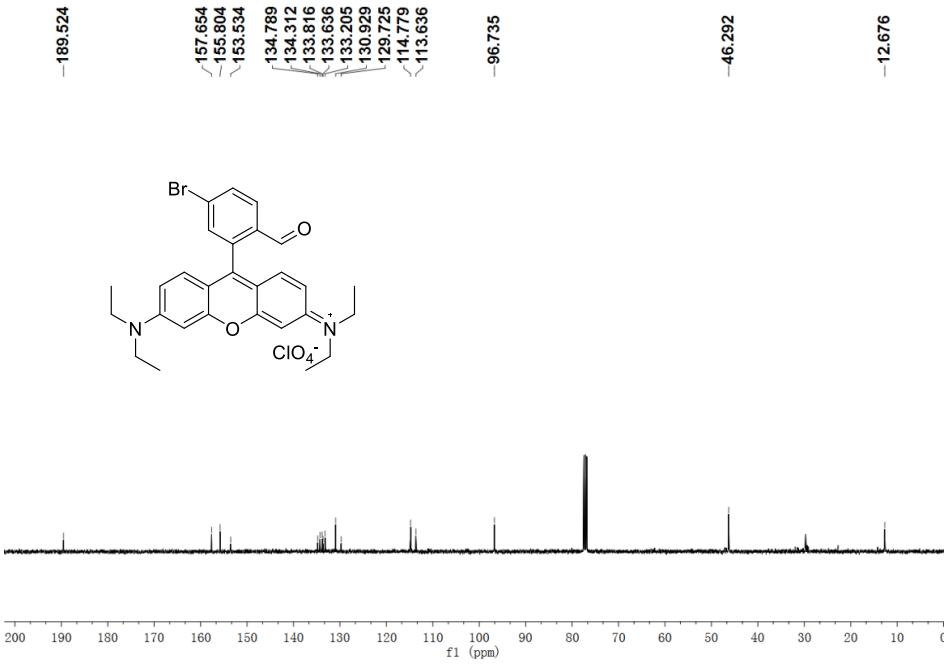
189.524
157.654
155.804
153.534
134.789
134.312
133.816
133.636
133.205
130.929
129.725
114.779
113.636
96.735
46.292
12.676
Br
O
N
O
N
ClO4-
f1 (ppm)

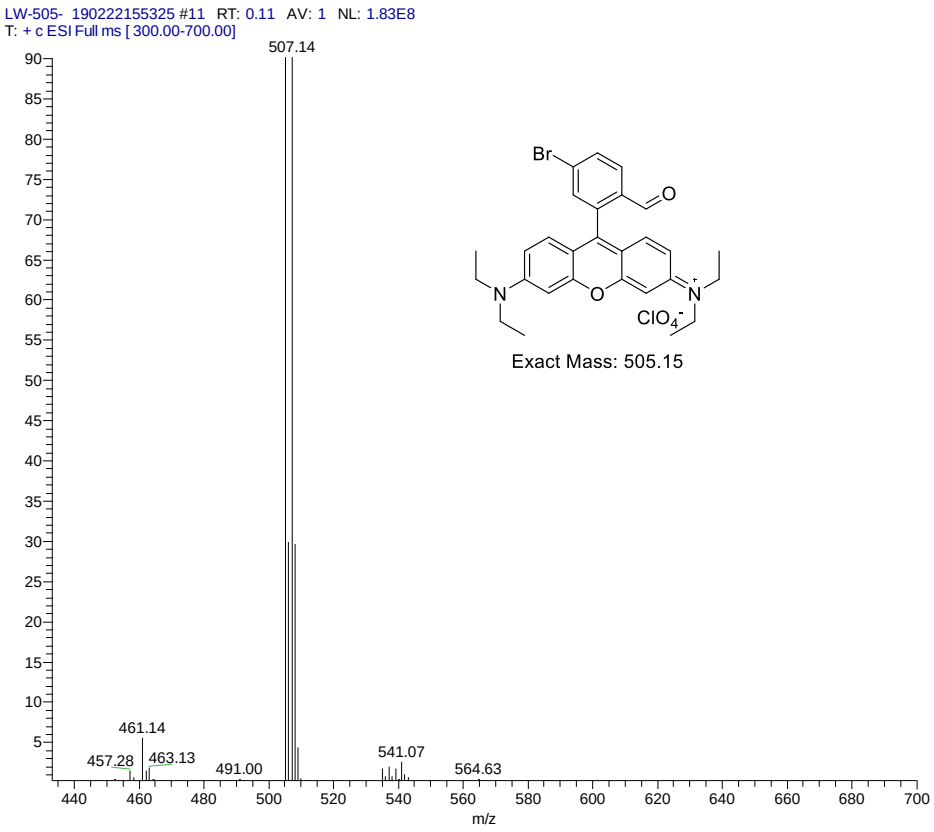
LW-505- 190222155325 #11 RT: 0.11 AV: 1 NL: 1.83E8
T: + c ESI Full ms [300.00-700.00]
507.14
461.14
457.28
463.13
491.00
541.07
564.63
m/z
Br
O
N
O
N
ClO4-
Exact Mass: 505.15

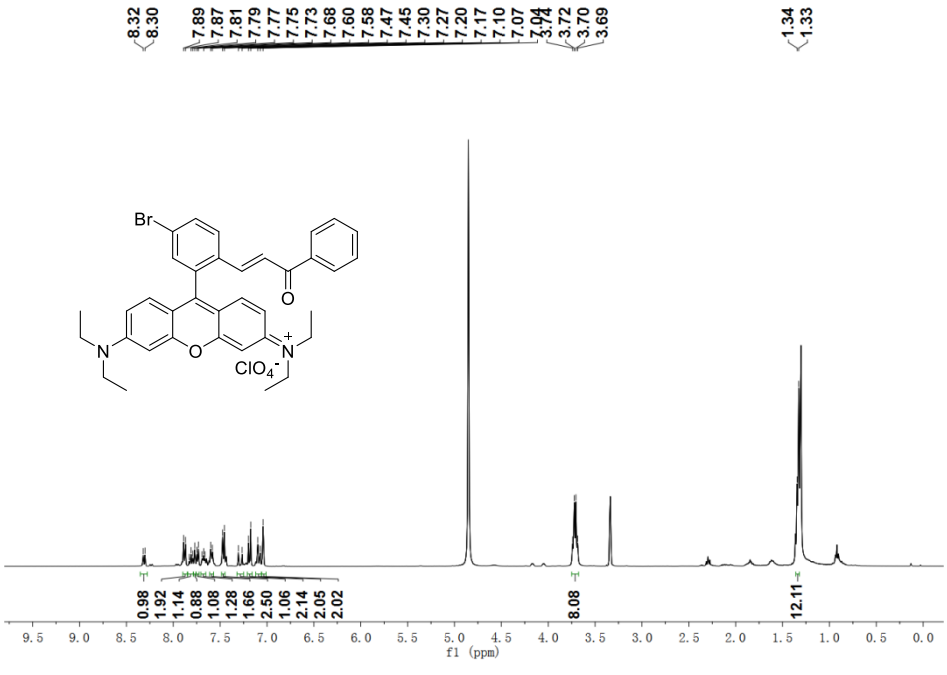
8.32
8.30
7.89
7.87
7.81
7.79
7.77
7.75
7.73
7.68
7.60
7.58
7.47
7.45
7.30
7.27
7.20
7.17
7.10
7.07
3.74
3.72
3.70
3.69
1.34
1.33
Br
O
N
O
N
ClO4-
0.98
1.92
1.14
0.88
1.08
1.28
1.66
2.50
1.06
2.14
2.05
2.02
8.08
12.11
f1 (ppm)

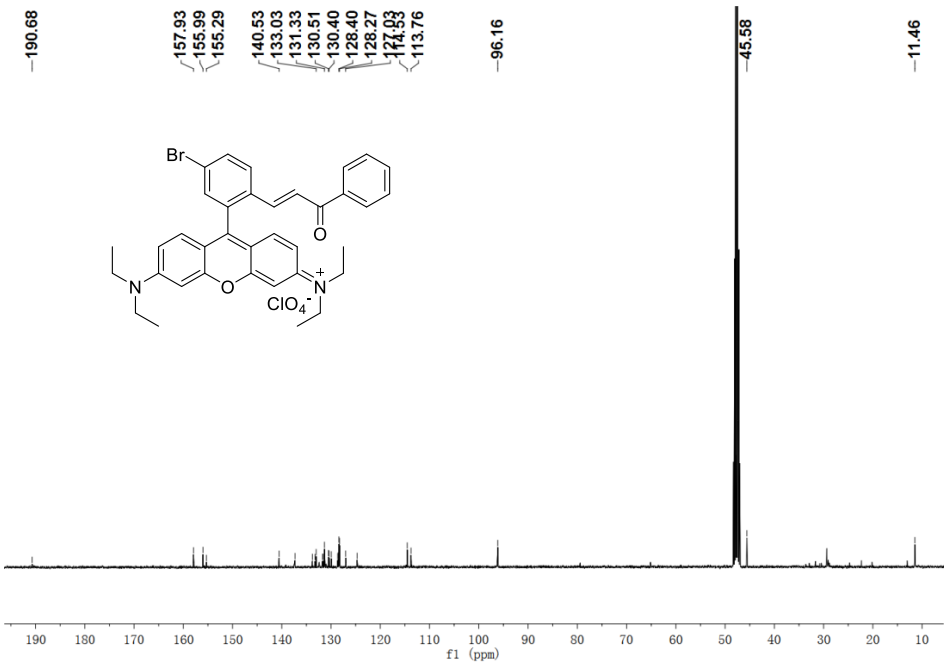
190.68
157.93
155.99
155.29
140.53
133.03
131.33
130.51
130.40
128.40
128.27
127.03
114.53
113.76
96.16
45.58
11.46
Br
O
N
O
N+
ClO4-
190 180 170 160 150 140 130 120 110 100 90 80 70 60 50 40 30 20 10
f1 (ppm)

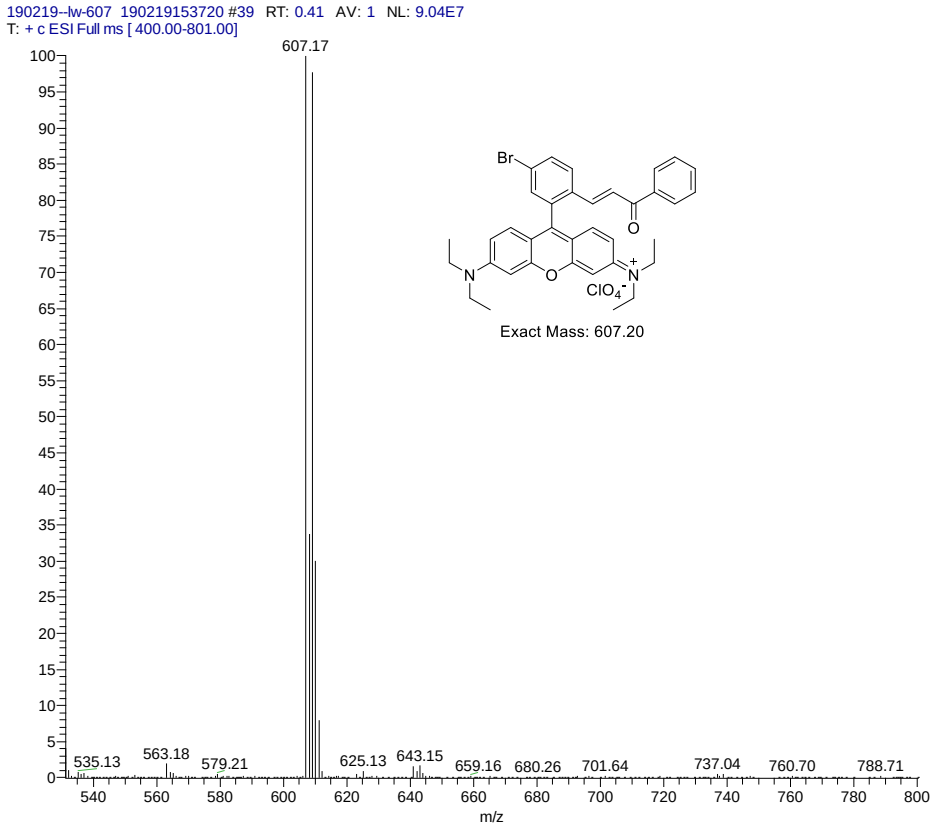
190219--lw-607 190219153720 #39 RT: 0.41 AV: 1 NL: 9.04E7
T: + c ESI Full ms [400.00-801.00]
607.17
535.13
563.18
579.21
625.13
643.15
659.16
680.26
701.64
737.04
760.70
788.71
Br
O
N
O
N+
ClO4-
Exact Mass: 607.20
m/z

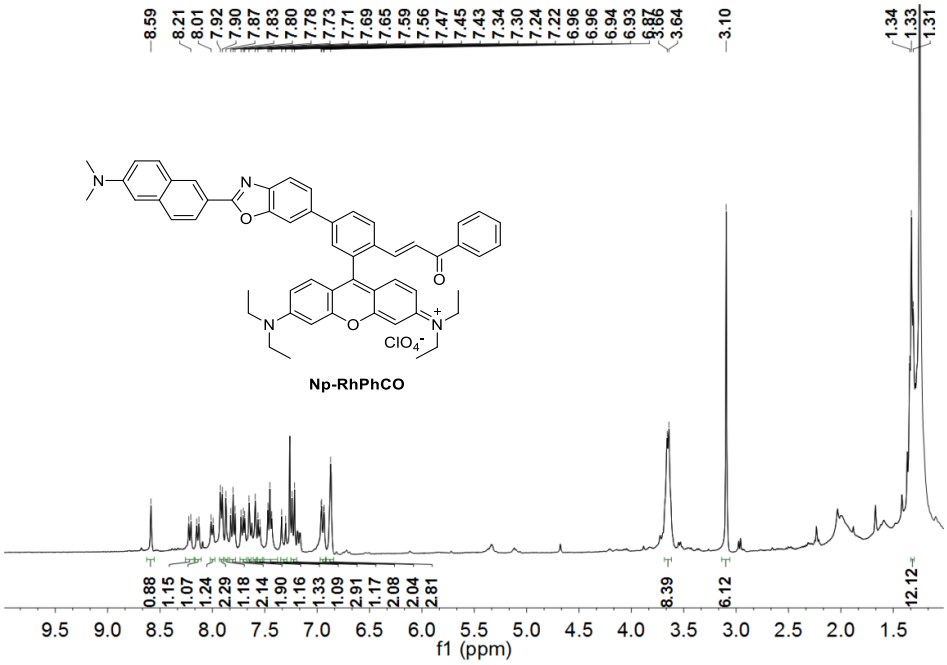
8.59
8.21
8.01
7.92
7.90
7.87
7.83
7.80
7.78
7.73
7.71
7.69
7.65
7.59
7.56
7.47
7.45
7.43
7.34
7.30
7.24
7.22
6.96
6.96
6.94
6.93
3.66
3.64
3.10
1.34
1.33
1.31
Np-RhPhCO
0.88
1.15
1.07
1.24
2.29
1.18
2.14
1.90
1.16
1.33
1.09
2.91
1.17
2.08
2.04
2.81
8.39
6.12
12.12
9.5 9.0 8.5 8.0 7.5 7.0 6.5 6.0 5.5 5.0 4.5 4.0 3.5 3.0 2.5 2.0 1.5
f1 (ppm)

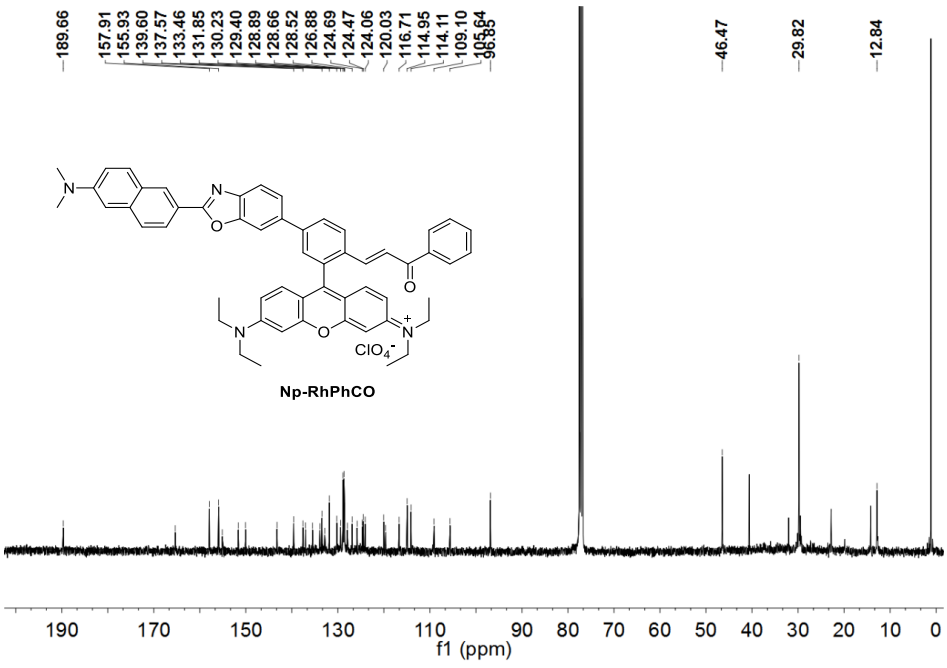
189.66
157.91
155.93
139.60
137.57
133.46
131.85
130.23
129.40
128.89
128.66
128.52
126.88
124.69
124.47
124.06
120.03
116.71
114.95
114.11
109.10
46.47
29.82
12.84
Np-RhPhCO
190 170 150 130 110 90 80 70 60 50 40 30 20 10 0
f1 (ppm)

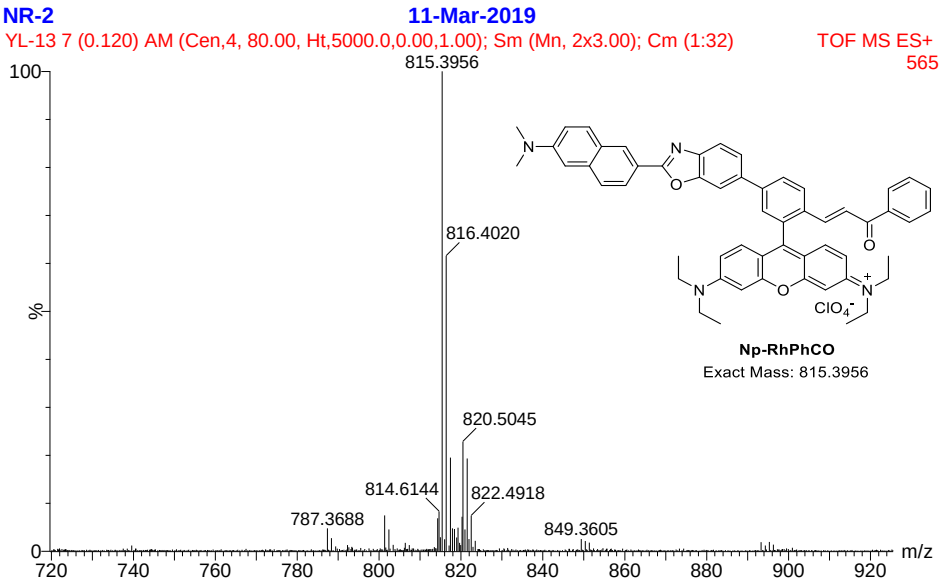
NR-2
11-Mar-2019
YL-13 7 (0.120) AM (Cen,4, 80.00, Ht,5000.0,0.00,1.00); Sm (Mn, 2x3.00); Cm (1:32)
TOF MS ES+
565
815.3956
816.4020
820.5045
814.6144
822.4918
787.3688
849.3605
100
%
0
720
740
760
780
800
820
840
860
880
900
920
m/z
Np-RhPhCO
Exact Mass: 815.3956